

Comparison of NCAR Community Climate Model (CCM) climates

James W. Hurrell

National Center for Atmospheric Research, PO Box 3000, Boulder, Colorado 80307, USA

Received: 27 December 1993/Accepted: 3 June 1994

Abstract. The simulated mean January and July climates of four versions of the National Center for Atmospheric Research (NCAR) Community Climate Model (CCM) are compared. The models include standard configurations of CCM1 and CCM2, as well as two widely-cited research versions, the Global Environmental and Ecological Simulation of Interactive Systems (GENESIS) model and the Climate Sensitivity and Carbon Dioxide (CSCO2) model. Each CCM version was integrated for 10 years with a horizontal spectral resolution of rhomboidal 15 (R15). Additionally, the standard T42 version of CCM2 was integrated for 20 years. Monthly mean, annually repeating climatological sea surface temperatures provided a lower boundary condition for each of the model simulations. The CCM troposphere is generally too cold, especially in the polar upper troposphere in the summer hemisphere. This is least severe in CCM2 and most pronounced in CCM1. CSCO2 is an exception with a substantial warm bias, especially in the tropical upper troposphere. Corresponding biases are evident in atmospheric moisture. The overall superior CCM2 thermodynamic behavior is principally compromised by a large warm and moist bias over the Northern Hemisphere middle and high latitudes during summer. Differences between the simulated and observed stationary wave patterns reveal sizeable amplitude errors and phase shifts in all CCM versions. A common problem evident in the upper troposphere is an erroneous cyclone pair that straddles the equatorial central Pacific in January. The overall January stationary wave error pattern in CCM2 and CSCO2 is suggestive of a reverse Pacific-North American teleconnection pattern originating from the tropical central Pacific. During July, common regional biases include simulated North Pacific troughs that are stronger and shifted to the west of observations, and each model overestimates the

strength of the anticyclone pair associated with the summer monsoon circulation over India. The simulated major convergence and divergence centers tend to be very localized in all CCM versions, with a tendency in each model for the maximum divergent centers to be unrealistically concentrated in monsoon regions and tied to regions of steep orography. Maxima in CCM-simulated precipitation correspond to the simulated outflow maxima and are generally larger than observational estimates, and the associated atmospheric latent heating appears to contribute to the stationary wave errors. Comparisons of simulated radiative quantities to satellite measurements reveal that the overall CCM2 radiative balance is better than in the other CCM versions. An error common to all models is that too much solar radiation is absorbed in the middle latitudes during summer.

1 Introduction

The National Center for Atmospheric Research (NCAR) Community Climate Model (CCM), a comprehensive three-dimensional global atmospheric general circulation model (AGCM), has been utilized by many university and NCAR scientists to study the Earth's climate system. Williamson (1993) reports that over 200 CCM-related investigations have appeared in the published literature since the inception of the CCM (CCM0) in 1982. However, as a result of continual model development at NCAR (which culminated in the release of CCM1 in 1987 and CCM2 in 1992), as well as modifications by individual scientists and their research groups, these investigations are based on several different versions of the CCM. It is the purpose of this study to compare some aspects of the simulated climates of four versions of the model. A much more detailed comparison is given in Hurrell et al. (1993). The models include two standard versions, CCM1 (Williamson et al. 1987) and CCM2 (Hack et al. 1993), and two research versions, the Global Environmental

Table 1. Resolution and major physical parameterization schemes in CCM2, CCM1, GENESIS and CSCO2

Model	Horizontal resolution	Vertical resolution	Convective scheme	Cloud scheme	Radiation scheme	Boundary-layer parameterization	Semi-Lagrangian transport	Diurnal cycle	Land surface	SST
CCM2	T42 R15	18 (hybrid)	Mass flux Hack (1994)	Kiehl et al. (1994)	δ -Eddington solar scheme Kiehl and Briegleb (1991) Briegleb (1992)	Yes	Water vapor + arbitrary number of fields Williamson and Rasch (1989, 1994)	Yes	Fixed soil moisture	Shea et al. (1992)
CCM1	R15	12 (sigma)	Moist convective adjustment	Ramathan et al. (1983)	Kiehl et al. (1987)	No	No	No	Fixed soil moisture	Alexander and Mobley (1976)
GENESIS	R15	12 (sigma)	Plume convection Kreitzberg and Perkey (1976)	Slingo and Slingo (1991)	Thompson et al. (1987)	Yes	Water vapor + arbitrary number of fields Williamson and Rasch (1989)	Yes	Land surface transfer model Pollard and Thompson (1994)	Alexander and Mobley (1976)
CSCO2	R15	9 (sigma)	Hybrid mass flux Albrecht et al. (1986) Meehl and Albrecht (1988)	Ramathan et al. (1983)	Ramathan et al. (1983)	No	No	No	15-cm bucket Washington and VerPlank (1986)	Alexander and Mobley (1976)

and Ecological Simulation of Interactive Systems (GENESIS) model (Thompson et al. 1987) and the Climate Sensitivity and Carbon Dioxide (CSCO2) model (Washington and Meehl 1993). GENESIS is derived from CCM1 and has been utilized in many paleoclimate and land-surface process studies, while CSCO2 is based on CCM0 and has been used for coupled model experimentation and carbon dioxide (CO_2) sensitivity studies. Thorough descriptions of each model are given in Hurrell et al. (1993), and a summary of the main physical parameterizations and the horizontal and vertical resolutions of the four CCM versions is provided in Table 1.

The validation and comparison of atmospheric model output are important parts of modeling research. Most early efforts were made in connection with numerical weather prediction forecasts, although recent increased interest in climate and climate-change processes has made clear the need for systematic and comprehensive comparisons of atmospheric climate-model simulations. The latter has generally been hindered by the greater computational resources required, as well as by the lack of clear experimental strategies, so that many early studies compared climate simula-

tions from uncoordinated and often dissimilar runs. Such comparisons are defined by the Working Group on Numerical Experimentation (WGNE) as level 1 comparisons, whereas simulations made under standard conditions validated against common data are referred to as level 2 comparisons (Gates 1992). The advantages of level 2 comparisons are clear, and this approach is becoming widely adopted.

Boer et al. (1991, 1992), for example, compared the climates simulated by 14 atmospheric models that had specified ocean surface temperatures and sea-ice boundaries based on climatological means. They grouped models of similar resolution and numerics into four categories, examined a few of the most basic circulation variables, and commented on apparent dependencies of the simulated climates on resolution and specific physical parameterizations. A similar comparison was performed by Gates et al. (1990, 1992) on global mixed-layer ocean-atmosphere models as part of the Intergovernmental Panel on Climate Change (IPCC) reports. Perhaps the most ambitious and comprehensive model comparison to date is the ongoing international effort of the Atmospheric Model Intercomparison Project (AMIP). As part of AMIP, approximately

30 different atmospheric climate models are simulating the decade 1979–1988 with specified but varying observationally-based boundary conditions (Gates 1992). A project such as AMIP may well serve as a prototype for future comparisons of fully-coupled ocean-atmosphere climate system models.

The results of comparisons are useful in that they can identify strengths and deficiencies common to different models. Moreover, since the various models have different numerical schemes, horizontal and vertical resolutions, and physical parameterizations, information on the effects of these differences are implicit in the results, although they are often difficult to identify clearly except in a most general way. Comparisons of different generations of models can also demonstrate evolutionary improvements, and those models that show favorable features in their simulated climate can be further studied to isolate and better understand the reasons for the improvements. Yet, given the enormous complexity of the models and the strong nonlinear coupling that exists among individual components of the models, the results of comparison projects may not readily translate into model improvements. Also, in order to judge properly the success of a model simulation, it is necessary that the validation examine many different fields since the success of any particular simulation can depend on the quantity chosen for comparison. This requirement demands extensive global data sets of high quality, a criterion that is difficult to meet for fields such as moisture, clouds and precipitation over the oceans. Despite these difficulties, the model-comparison approach yields valuable information about model behavior, and with an ever-increasing emphasis on the development of comprehensive climate system models, such evaluations are necessary to determine which atmospheric models are most suitable to serve as components of a climate system model.

This study presents a comparison of four different versions of the CCM, and it serves as a brief summary of a much more detailed comparison given by Hurrell et al. (1993). The motivation behind their work was not only to validate the CCM versions, and thereby document common strengths and deficiencies as well as evolutionary improvements, but also to provide a benchmark against which future CCM versions could be measured. A benefit of their effort was that a documentation of the circulation statistics of different CCM versions was provided under one cover for the first time. Currently, no comparable documentation of the climates of either CSCO2 or GENESIS exists, while some seasonal and perpetual January and July summary statistics are given in Williamson and Williamson (1987) for CCM1. Some aspects of the CCM2 climate have recently been documented by Hack et al. (1994) and Kiehl et al. (1994).

Each CCM version was integrated for 10 years with a horizontal spectral resolution of rhomboidal 15 (R15), including a low-resolution R15 version of CCM2. Additionally, the standard CCM2 configuration was integrated for 20 years with a horizontal spectral resolution of triangular 42 (T42). Some informa-

tion on the resolution dependence of the CCM2 climate is, therefore, contained in the results, although a more detailed study of the impact of resolution on CCM2 simulations is presented by Williamson et al. (1994). Annually repeating climatological monthly mean sea surface temperatures (SSTs) provided a lower boundary condition for each seasonal-cycle integration. Because CCM2 utilizes the SST climatology of Shea et al. (1992), while CCM1, GENESIS and CSCO2 utilize the climatology of Alexander and Mobley (1976), this comparison is not strictly a level 2 comparison as defined by the WGNE.

2 Validation data

2.1 ECMWF analyses

Many different fields are examined in Hurrell et al. (1993) in an attempt to gain a fairly complete view of each simulation. The primary source of validation data is the European Centre for Medium Range Weather Forecasts (ECMWF) global analyses, which are believed to be the best operational global analyses available for general use (Trenberth and Olson 1988; Trenberth 1992). For climate studies, a major concern is the impact of operational changes in the analysis-forecast system employed at ECMWF to produce the analyses. It is important to know in detail the effects of the changes and the resulting biases that may exist. A comprehensive evaluation of the ECMWF global analyses is given by Trenberth (1992), who also discusses the usefulness of the analyses for climate studies.

Two archived data sets from ECMWF are used to verify the simulated climates, both of which are described in detail by Trenberth (1992). The first is the WMO¹ archive, which consists of twice-daily, initialized analyses at seven pressure levels in the vertical. Eleven-year (1979–1989) January and July climatologies were constructed from this archive for fields that were minimally affected over this time by the operational changes at ECMWF. Fields associated with moisture and the divergent component of the wind, however, clearly exhibit spurious trends over these years (e.g., see Figs. 35–41 in Trenberth 1992). For these variables, the WCRP/TOGA² archive was used, which begins in 1985 and consists of four times daily, uninitialized analyses at fourteen pressure levels in the vertical. Climatologies over the relatively short periods of January 1987–1989 and July 1986–1988 were constructed from this archive. These periods, which were also shown by Trenberth (1992), come after a major change in May 1986 and before a major change in May 1989.

¹ World Meteorological Organization

² TOGA (Tropical Oceans Global Atmosphere) is a program under the World Climate Research Programme (WCRP)

2.2 Satellite data

Satellite data for climate monitoring have become increasingly available over the past decade and they provide another important source for validating climate models. To examine the radiative budgets of the models, data from the Earth Radiation Budget Experiment (ERBE) are utilized. The ERBE is a multisatellite project that measures the broadband components of the earth's radiation balance to a high degree of accuracy with diurnal resolution (e.g., Barkstrom et al. 1989). Yet, because the ERBE data products are complex combinations of data and models, their uncertainties are difficult to assess. Barkstrom et al. (1989) estimate that regional monthly averages have uncertainties of $\pm 5 \text{ W m}^{-2}$ for both the shortwave and longwave channels. The uncertainty in the global annual average net radiation is also about $\pm 5 \text{ W m}^{-2}$, an estimate based on the differences of four "validation" months that were intensively analyzed by the ERBE Science Team (1986). The fundamental radiometric accuracy of the individual radiances is high, but the need for radiance to flux conversion (inversion) and diurnal and monthly averaging leads to most of the error. The ERBE climatologies include the periods January 1986–1989 and July 1985–1988 and are obtained from the S-4 data products, which are monthly shortwave and longwave fields.

The total cloud fields from the models are compared with total cloud-coverage estimates obtained from the International Satellite Cloud Climatology Project (ISCCP). ISCCP was established to use operational satellite data to produce a calibrated and normalized infrared (IR) and visible (VIS) radiance data set from which global, reduced-resolution cloud properties could be derived. Rossow and Schiffer (1991) and Rossow and Garder (1993a, b) describe the ISCCP cloud-analysis procedure in detail. The overall accuracy of the cloud data is difficult to assess because the definition of a cloud is inherently an arbitrary radiance-threshold test. Other uncertainties are introduced by the movement and failure of satellites, limb darkening, and daily weather fluctuations that affect the monthly mean estimates of cloud amount. The global annual mean total cloud amount estimated from ISCCP data is $\approx 63\%$ (e.g., Hurrell and Campbell 1992; Rossow et al. 1993), which is about 10% higher than simultaneous measurements obtained from the Nimbus-7 Cloud matrix (Stowe et al. 1988, 1989) climatology. Other older climatologies are in better agreement with the lower Nimbus-7 estimates (Hughes 1984), although earlier measures of total cloud cover may be lower partly because of incomplete global coverage. The ground-based climatology described by Warren et al. (1986, 1988) reports a global annual mean cloud amount near 61%, which is closer to the ISCCP estimate. The climatologies of total cloud from ISCCP cover the periods January 1984–1991 and July 1983–1990 and are taken from Stage C2 data, which consist of monthly averaged cloud properties.

2.3 Precipitation

One variable of great interest is precipitation, which is extremely difficult to measure globally, especially over vast uninhabited areas such as the oceans. The data used are from the climatology of Legates and Wilmott (1990). Their monthly estimates of precipitation are made from nearly 25000 land stations, although the overwhelming majority are from the United States, southern Canada and Europe (see their Fig. 1). Oceanic precipitation was estimated according to Dorman and Bourke (1978) by an empirical relationship between monthly rainfall totals and the "current weather" recorded on board ships. Comparisons between the Legates and Wilmott precipitation estimates and the climatologies of Jaeger (1983) and Shea (1986) show generally good agreement over land, but differ considerably over the oceans, especially over the tropical Pacific where direct measurements do not exist (Shea, personal communication). Thus, comparisons with model output over these regions are qualitative at best.

3 Results

Many results are presented in six-panel figures for both mean January and July simulated climates. The format is to present the validation data in the first panel, followed by fields from the CCM2 (T42 and R15), GENESIS, CCM1, and CSCO2 simulations. Subtracting observed from simulated fields highlights the differences between them and the differences between individual models, so difference maps will be presented for most variables. The results shown here are only a sample of those presented in Hurrell et al. (1993), where many climate variables were examined in order to provide a better-balanced and more complete view of the models' ability to simulate the observed climate.

3.1 Temperature

Perhaps the most basic of all climate parameters is temperature. All versions of the CCM simulate the broad structure of the observed zonal temperature distribution with its strong variation with height and latitude. Of errors common to many AGCMs, the most notable is the general coldness of the simulated atmosphere. This is true of the CCM versions too, especially in the polar upper troposphere and lower stratosphere in the summer hemisphere. The cold polar tropopause represents a pervasive and persistent problem in atmospheric general circulation modeling (Boer et al. 1992). Although a characteristic feature in all versions of the CCM, it is noticeably smaller in the CCM2 simulated climate (Figs. 1 and 2). In the lower and middle troposphere in tropical and middle latitudes, CCM2 simulated temperatures are generally too cold by 1–2°C, compared with cold biases of up to 3–4°C in GENESIS and CCM1. An exception is the middle latitudes of the

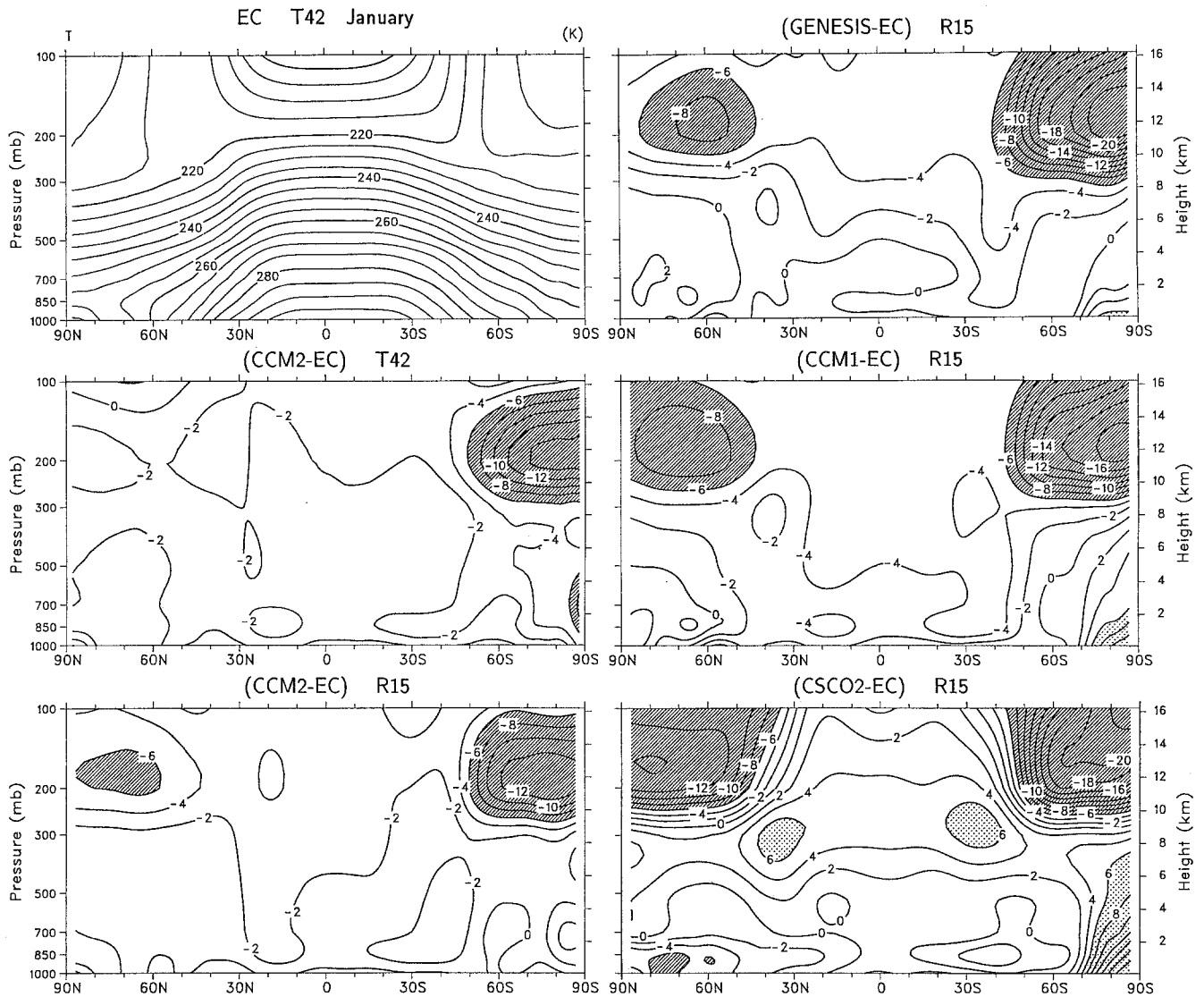


Fig. 1. Zonally-averaged mean January temperature (K) from ECMWF, and differences from the ECMWF climatology for each CCM simulation. Differences are contoured in increments of

2 K with values greater than 6 K shaded and less than -6 K hatched

Northern Hemisphere (NH) during summer where CCM2, GENESIS and CSCO2 exhibit a warm bias that is most pronounced over landmasses. CSCO2 also exhibits a pronounced warm bias at higher levels and throughout the depth of the tropics where simulated temperatures exceed ECMWF values by more than 6° C near 300 mb.

3.2 Moisture

Zonally-averaged profiles of precipitable water are shown in Fig. 3. Recall that for moisture variables, the ECMWF climatologies represent the relatively short periods of January 1987–1989 and July 1986–1988. Given the large uncertainty in the analyzed moisture field, as evidenced by the large changes in the post May 1989 analysis cycle (e.g., Trenberth 1992; Kiehl and Briegleb 1992), the moisture biases reported in this section are

useful for illustrating similarities in the behavior of the various CCM versions, but should not be viewed as a definitive quantification of model errors.

In the tropics during both January and July, CSCO2 is too moist and the other models are too dry, with CCM2 matching the ECMWF estimates the most closely and CCM1 being the driest (Fig. 3). Zonally-averaged cross-sections of specific humidity (not shown) reveal that all CCM versions are dry relative to the ECMWF data in the lower tropical troposphere (850 mb and below), and this bias is especially large in CCM1 where it extends to higher levels as well. In contrast, most of the tropical troposphere above 850 mb is too moist in CSCO2, especially near 700 mb where specific humidities are too large by nearly 60%. CCM2 and GENESIS are too moist near 700 mb in the tropics and subtropics, and both models are dry compared with the ECMWF analyses above that level. Also evident in Fig. 3 is a moist bias in the middle latitudes of

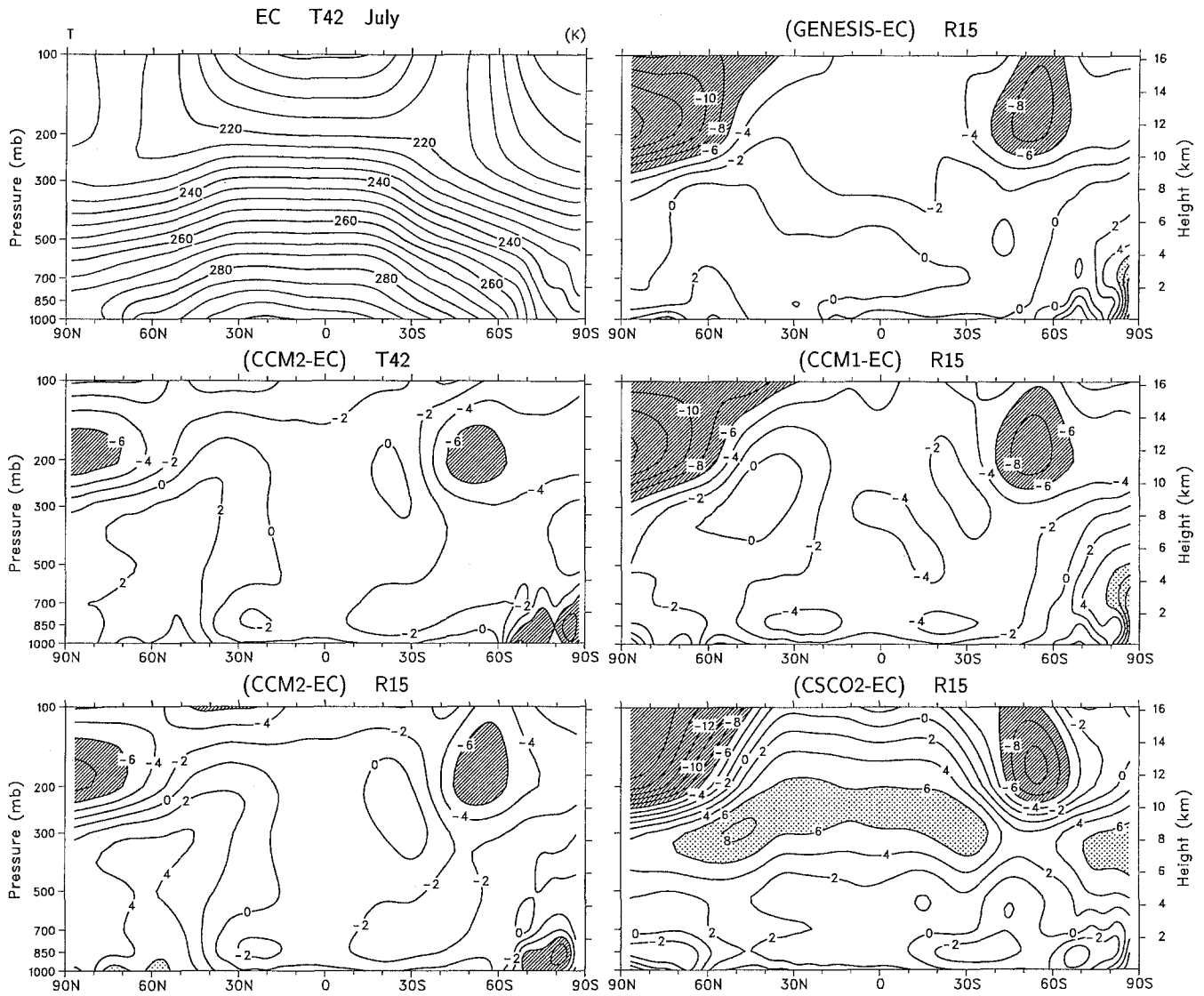


Fig. 2. As in Fig. 1, but for July

the NH during summer. This error, which is largest in CCM2, is consistent with the warm biases noted earlier.

Another way to examine moisture is through plots of relative humidity. Since the water-holding capacity of the atmosphere is strongly tied to temperature, patterns of specific humidity biases generally follow patterns of temperature biases. Moreover, through feedbacks associated with the greenhouse effect of water vapor, low values of specific humidity are associated with cold temperatures and vice versa. Thus, an examination of relative humidity can reveal information not contained in plots of specific humidity, and relative humidity is a key parameter in diagnosing clouds. Relative humidity is analyzed at and below 300 mb at ECMWF, so values in the upper troposphere are not presented.

Zonally-averaged cross-sections of relative humidity are shown in Figs. 4 and 5. All CCM versions have simulated humidities that are generally less than analyzed values in the lower troposphere over the tropics.

The largest differences from the ECMWF climatological values are evident in CCM1 and CSCO2 at high latitudes where simulated humidities are too low, especially in the winter hemisphere. In the middle troposphere, CSCO2 significantly overestimates the relative humidity over the tropics, while the other CCM versions tend to have lower simulated humidities than analyzed. Regionally, a common bias is that CCM relative humidities are less than ECMWF values over marine stratus regimes (not shown). These biases are most evident in CCM1 and are least pronounced in CCM2. Otherwise, there are relatively few features common to the simulations, although there is a remarkable similarity between January and July biases in each model.

3.3 Sea-level pressure

The mean sea-level pressure (SLP) pattern is a useful indication of a model's ability to simulate the atmos-

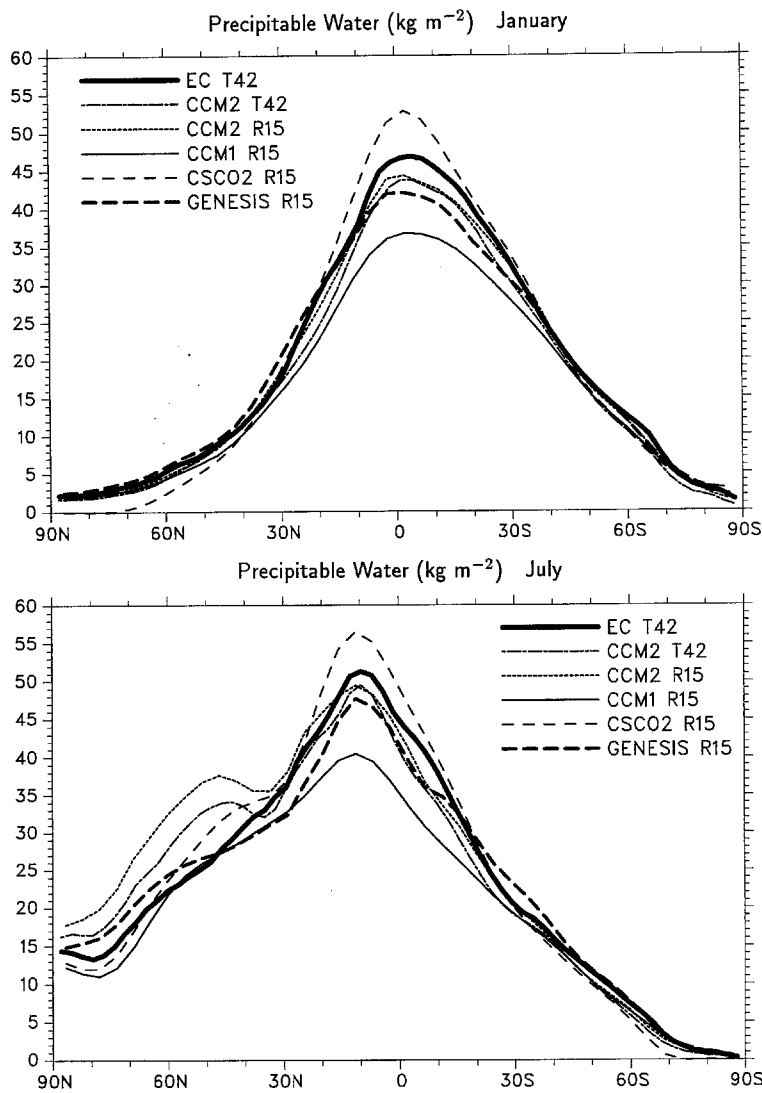


Fig. 3. Zonally-averaged mean precipitable water (kg m^{-2}) for January (*top*) and July (*bottom*)

pheric circulation near the surface, and it represents an integrated measure of a model's thermodynamic and dynamic representations. The zonally-averaged SLP fields are shown in Fig. 6, and the spatial distribution of regional differences from ECMWF data are presented in Figs. 7 and 8. All CCM versions reproduce the basic observed patterns, the Siberian high and Aleutian and Icelandic lows during NH winter (Fig. 7), subtropical ridges, and the Southern Hemisphere (SH) circumpolar trough. Large regional errors, however, are prevalent. January SLPs in CCM2 at T42 resolution are lower than the ECMWF analyses over most of Europe, Asia, North America and the North Atlantic, and higher over North Africa. The Aleutian low is too weak and is displaced westward, which accounts for an SLP error of more than 12 mb over the eastern North Pacific. This pattern is consistent with regional temperature errors (not shown), with anomalous northerly cold advection over the west coast of North America and southerly warm advection over the central and western Pacific. The problem in the North Pacific is not as evident in CCM2 at R15 resolution. The Aleutian low is also poorly simulated in CSC02 where, in

this case, SLPs are erroneously high throughout the middle latitudes of the NH and are too low over high latitudes. SLPs in GENESIS are generally too high everywhere, except the North Atlantic where the Icelandic low is too deep and is displaced to the southeast. The CCM1 January simulation also shows large regional differences from the ECMWF analyses, especially in high northern latitudes and in the SH subtropics, where the subtropical ridges are too weak by 4 to 8 mb. The SH subtropical ridges in CCM2 T42 are too strong and are displaced poleward, while pressures near the circumpolar trough tend to be lower than observed.

The dependence of the simulation of the circumpolar trough on resolution has been noted in other comparison studies (e.g., Gates et al. 1990; Boer et al. 1991). The R15 resolution versions of the CCM severely underestimate the strength of the trough and place it too far equatorward, and these errors are present during both southern summer and winter. Tzeng et al. (1993) showed that the errors in the latitudinal location and intensity of the circumpolar trough simulated by the CCM1 were mainly due to the low horizontal

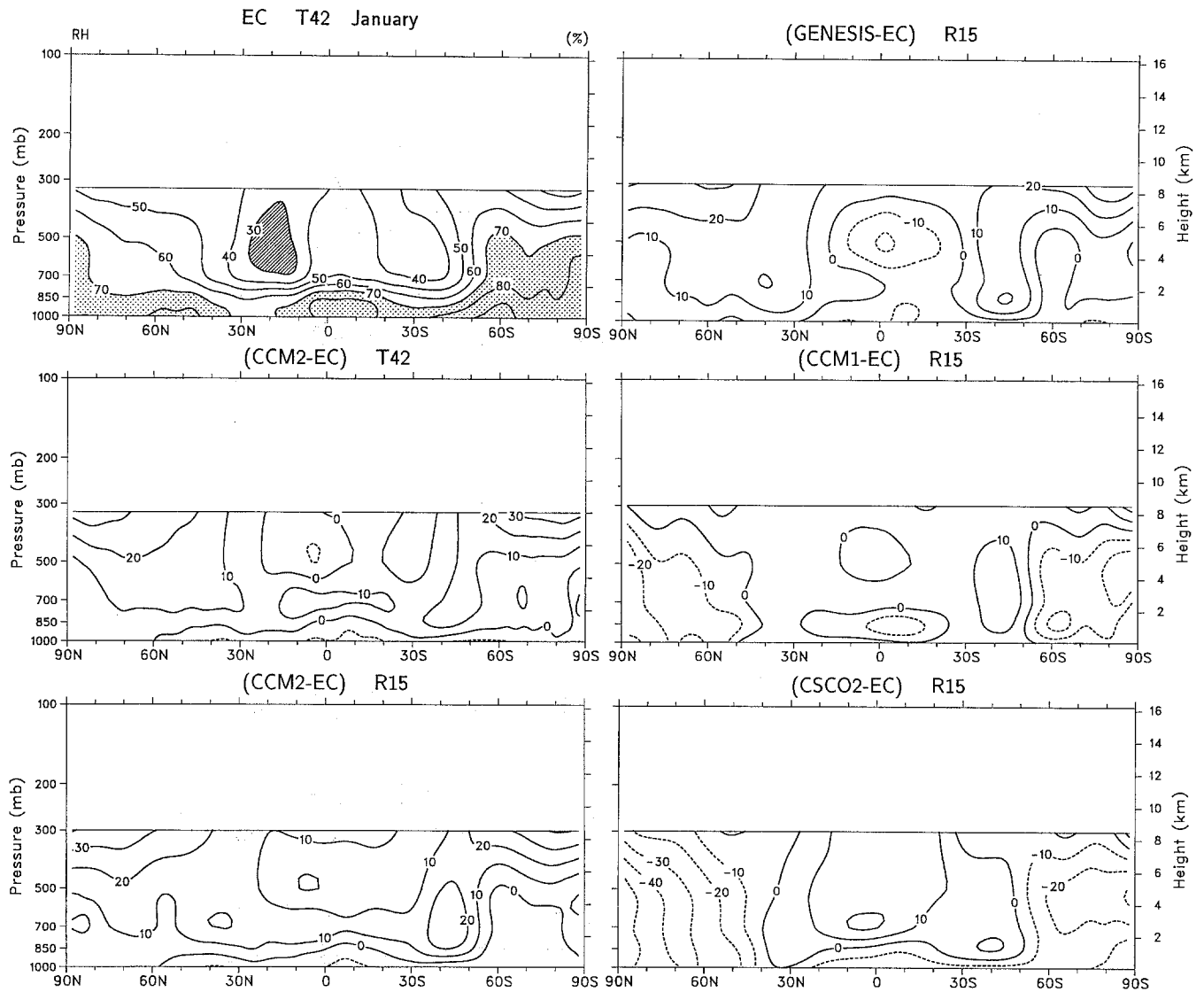


Fig. 4. Zonally-averaged mean January relative humidity from ECMWF, and differences from the ECMWF climatology for each CCM simulation. The ECMWF values are contoured every 10%,

with values greater than 70% shaded and values less than 30% hatched. Differences are contoured in increments of 10% and negative values are dashed

resolution of the model, and the results of Williamson et al. (1994) corroborate this finding for the CCM2. The large CCM2 T42 SLP errors in high SH latitudes during July result from the circumpolar trough being too deep and too far equatorward. In the NH, the summer subtropical ridges over the Pacific and Atlantic in CCM2 are too strong and pressures over the landmasses tend to be too low. Similar biases exist in CSCO2, and SLPs in the tropical western Pacific are too low by nearly 6 mb. As for January, GENESIS simulated SLPs are biased too high nearly everywhere. It turns out that this systematic bias in GENESIS is related to an incorrect specification of surface topography. The globally-averaged surface height in GENESIS is 308.7 m, compared with 230.1 m in CCM1, for example, and an observed value of 237.3 m. Therefore, while the globally-averaged mean surface pressure is near 985 mb in both GENESIS and CCM1, the global value of mean SLP has a positive bias of nearly 9 mb in

GENESIS. Moreover, this bias in SLP is reflected at 500 mb by a global-mean geopotential height bias of nearly 70 m.

3.4 Wind

The horizontal wind distribution is closely linked geostrophically to the temperature and pressure distributions. The zonal wind, in particular, has traditionally been one of the fundamental climate simulation verification parameters. Regional features of the flow at 200 mb are shown in Figs. 9 and 10. In January, the major features of the zonal flow are qualitatively well simulated by each model, including the westerly maxima off the east coasts of Asia and North America, broad regions of tropical easterlies, the tropical eastern Pacific westerly maximum at 200 mb, and a summer westerly maximum in middle latitudes of the SH. The

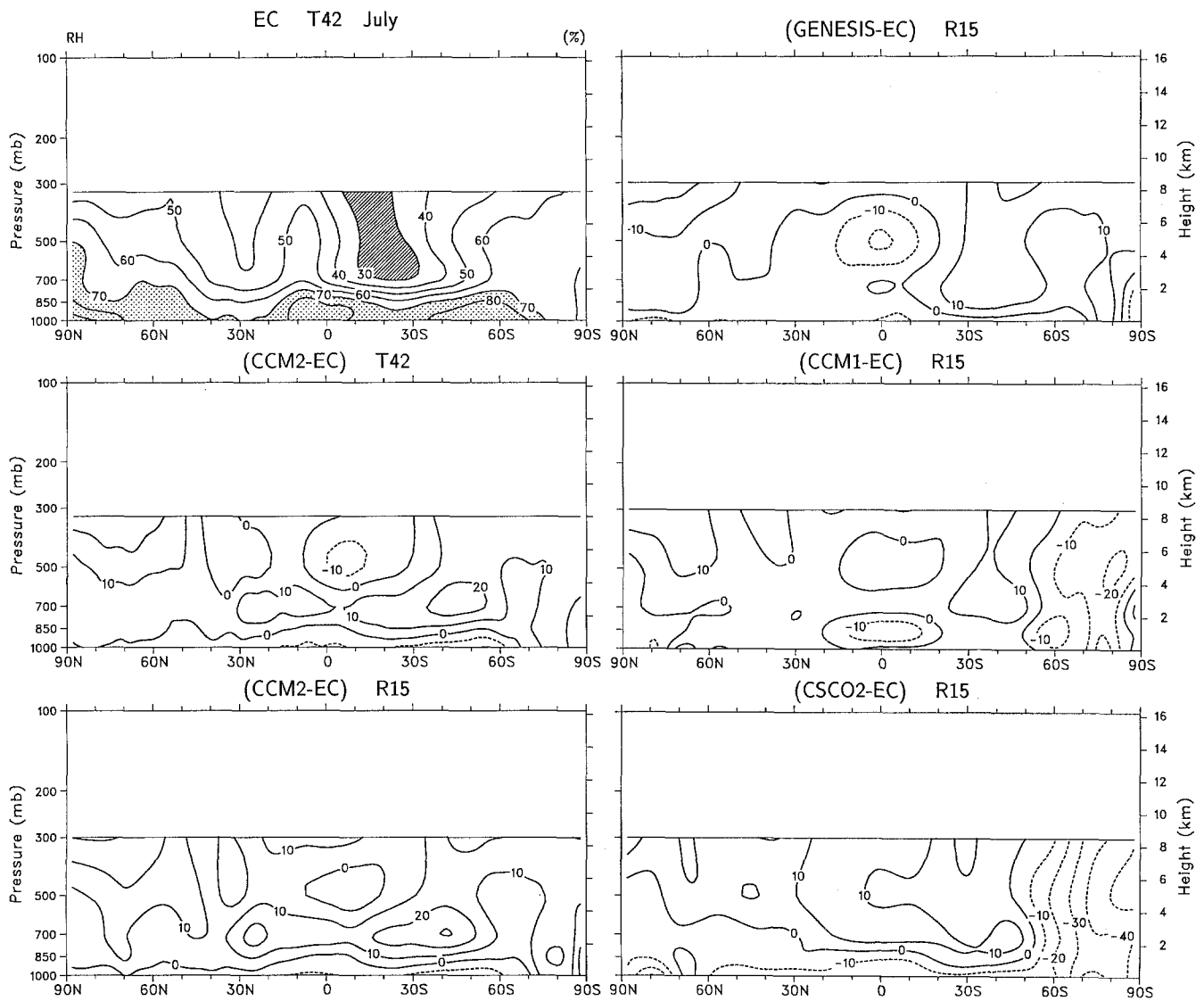


Fig. 5. As in Fig. 4, but for July

latter is generally too weak and too far equatorward, especially in the R15 models, and is slightly stronger and more extensive than observed in CCM2 T42. These errors at high latitudes of the SH are consistent with biases in the SLP (Fig. 7) and 500 mb height fields (not shown). In the tropical central Pacific, westerly biases of large amplitude are evident at 200 mb in all CCM versions. This error represents both an in-phase westerly bias and a westward shift of the models' tropical westerly flow regime relative to the ECMWF analyses. In the NH extratropics, the largest regional biases are over the Pacific, in particular the east Asian jet being weaker and more contracted in the model simulations than in the analyses. In the lower troposphere at 850 mb (not shown), the easterlies across the tropical central Pacific are too strong in each CCM version, with easterly biases of more than -7 m s^{-1} in CCM2 and -12 m s^{-1} in CSCO2.

The westerly bias at 200 mb over the central tropical Pacific is also evident in each CCM version during July (Fig. 10). Another common error during northern sum-

mer is that the easterlies over North Africa and Asia extend too far north and are too strong in each model. The simulated westerly maximum over Australia differs among the models, and the general tendency is for an easterly bias to extend across central Australia into the Pacific and a westerly error over southern Australia to extend across New Zealand where the local minimum is not well simulated. At 850 mb (not shown), notable problems in the tropics include simulated easterlies that are too strong across the Pacific, especially in CCM2 and CSCO2, and strong erroneous low-level convergence in CCM2 and GENESIS over Central America. The 850 mb SH westerly maxima in middle and high latitudes tend to be shifted equatorward in GENESIS, CCM1 and CSCO2, resulting in easterly biases centered near 55°S .

3.5 Rotational flow

The rotational component of the flow, as depicted by the streamfunction, is a well measured quantity. More-

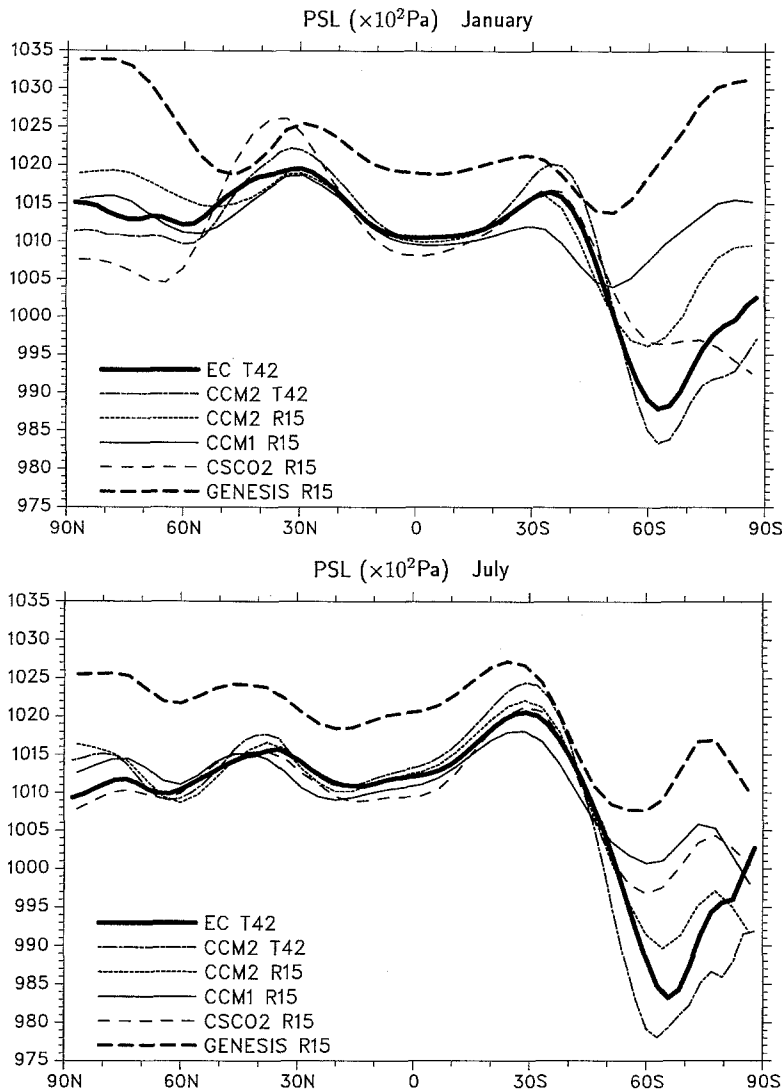


Fig. 6. Zonally-averaged mean sea-level pressure ($\times 10^2$ Pa) for January (*top*) and July (*bottom*)

over, by examining departures from the zonal symmetry (i.e., the eddy streamfunction), stationary wave patterns extending through the tropics can be examined. Regional differences between the simulated and observed eddy streamfunction at 200 mb are shown in Figs. 11 and 12.

All CCM versions qualitatively reproduce the major circulation centers. In January in the upper troposphere, these include the low-latitude anticyclonic couplet that straddles the equator in the west Pacific, the tropical cyclonic centers over the east Pacific and Atlantic, and the major ridges and troughs in middle latitudes of the NH (Fig. 11). In July, the main upper-tropospheric features reproduced by all CCM versions include the anticyclonic centers associated with the Indian summer monsoon circulation and the subtropical troughs in the Pacific and Atlantic Oceans (Fig. 12). Phase shifts and sizeable amplitude errors, however, result in large regional biases; many of which are common to the different CCM versions.

One example of a common problem is an erroneous cyclone pair that straddles the equatorial central Pacific in January (Fig. 11). This feature, which is less

pronounced in CCM1, results from a westward shift of the subtropical stationary wave troughs relative to observations, and it is consistent with the large equatorial central Pacific westerly wind bias noted at 200 mb in Fig. 9. Moreover, the overall error pattern in CCM2 and CSCO2 is suggestive of a reverse Pacific-North American (PNA) teleconnection originating from anomalous heating in the central equatorial Pacific. GENESIS, CCM1 and CSCO2 each exhibit different stationary wave biases over the PNA region. Large regional biases common to the different CCM versions are also evident during July (Fig. 12). Examples include the subtropical North Pacific troughs, which, as in January, are stronger and shifted to the west of observations, and the overestimation and misplacement of the anticyclone pair associated with the summer monsoon circulation over India.

3.6 Irrotational flow

The divergent component of the wind plays a much more prominent role in the tropics than in higher lati-

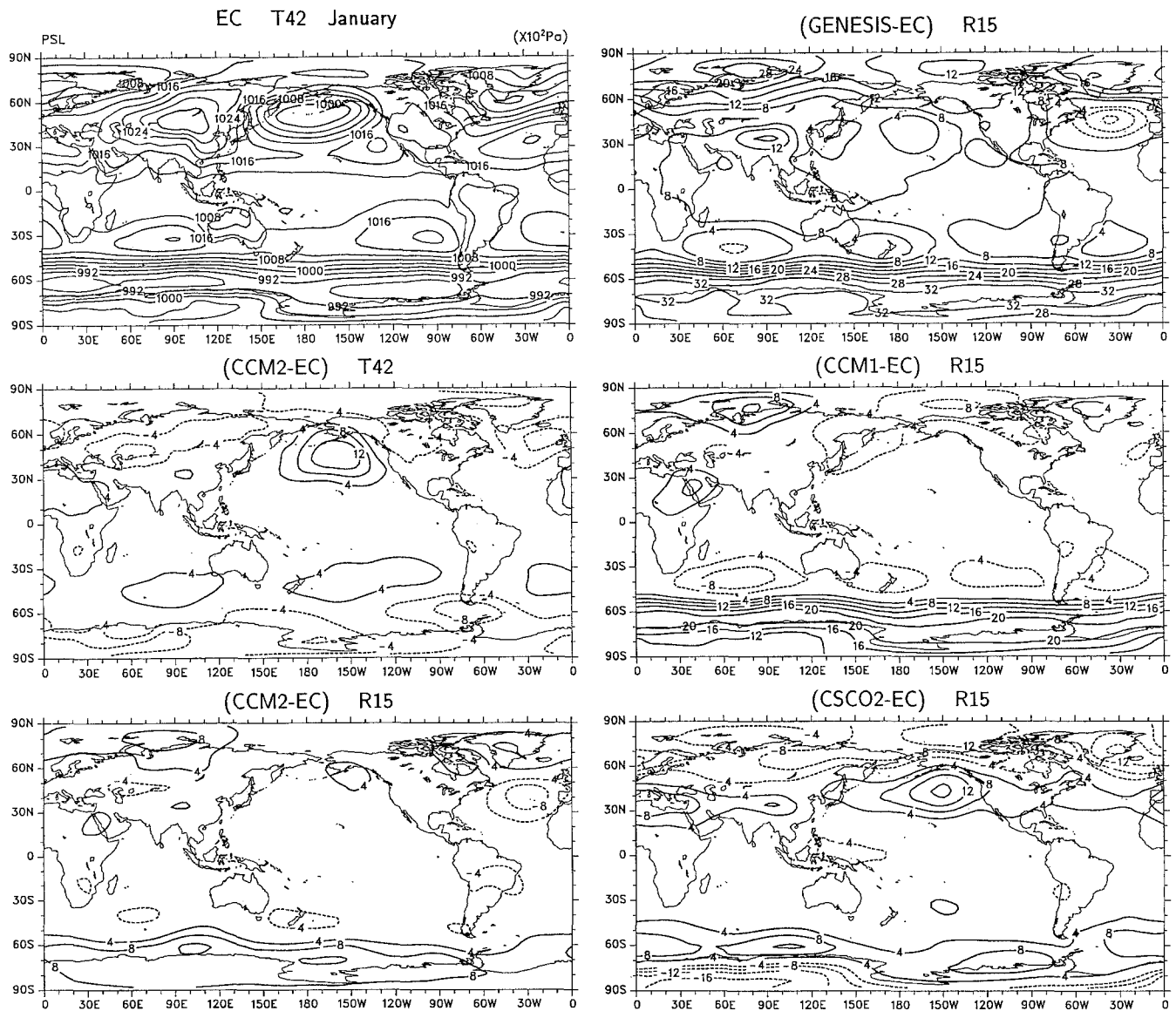


Fig. 7. Mean January sea-level pressure from ECMWF, and differences from the ECMWF climatology for each CCM simulation. The contour increment is 4 mb, negative values are dashed and the zero contour has been suppressed for clarity

tudes. The analysis of observed divergence is sensitive to the numerical prediction model used for the data assimilation and, in particular, to the parameterizations of convection used in the assimilating model. Biases introduced into the ECMWF analyses over time by changes to the forecast model and data-assimilation scheme have been documented by Trenberth (1992). Trenberth and Olson (1988) compared global analyses from the National Meteorological Center (NMC) and ECMWF, but since large discontinuities in time have also occurred at NMC, the interpretation of results is complicated. Nonetheless, it is generally true that, while the magnitude of the analyzed divergent wind (or vertical motion) has shown large changes over time, the general patterns of divergence are more robust. With this in mind, the ECMWF climatology is derived from the relatively short periods of January 1987–1989 and July 1986–1988.

The local divergent wind component and velocity potential at 200 mb are shown in Figs. 13 and 14. Note that total fields are presented and not difference maps, and vectors are plotted every third gridpoint on the T42 maps and every second gridpoint on the R15 maps. Perhaps the most noticeable feature is that the major convergence and divergence centers tend to be much more localized in the CCM versions than in the analyses, especially during northern winter. For example, the upper-tropospheric January tropical outflow in the ECMWF analyses extends zonally from the Indian Ocean to well east of the dateline, whereas each CCM version tends to limit very strong divergence to the New Guinea region (Fig. 13). The result is that, compared to the analyses, there is an enhanced Walker circulation resulting in upper-tropospheric convergence over the Indian Ocean and the central Pacific. These results also imply smaller heat sources over the central

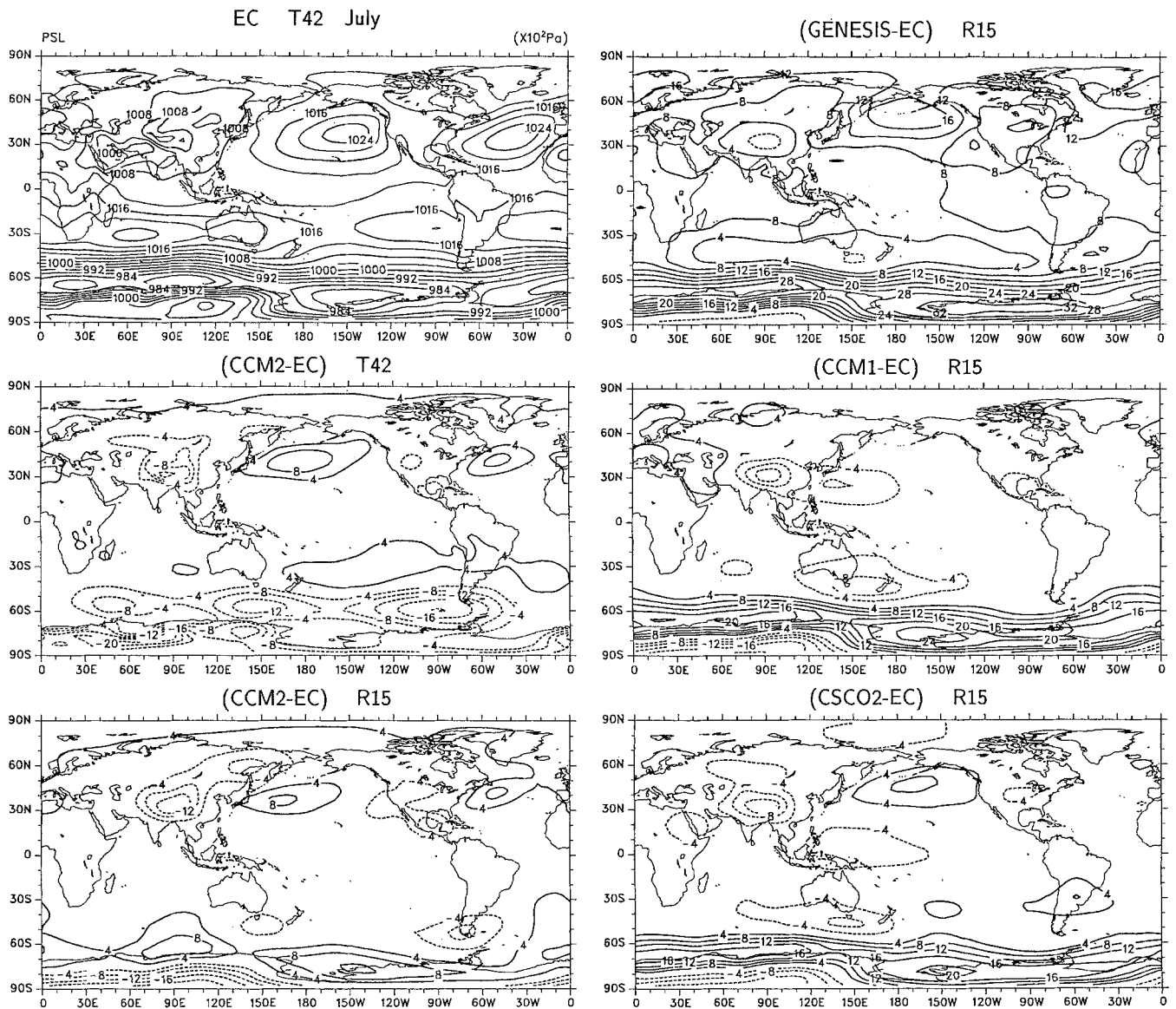


Fig. 8. As in Fig. 7, but for July

Pacific in the models, which would be consistent with the erroneous cyclone pairs and the stationary wave errors noted in the streamfunction fields (e.g., Fig. 11) and the westerly wind errors noted in Fig. 9. In general, there is a pronounced tendency in each CCM version for the divergent centers to be unrealistically concentrated in monsoon regions and sometimes tied to regions of steep orography.

Similar problems are noted during July. In particular, a broad area of upper-level divergence in the ECMWF analyses extends from the Indian summer monsoon region well across the central Pacific (Fig. 14). In the CCM versions, the center of outflow is much more localized and is generally stronger than analyzed, again resulting in much weaker upper-tropospheric divergence over the tropical central Pacific and Indian Ocean. Excessive low-level convergence is evident over Central America in CCM2, GENESIS and CCM1 (not shown), and the upper-level outflow

over this region is much stronger than in the ECMWF analyses, especially in the CCM2 simulation. CSCO2 has a striking global pattern of erroneously strong 200 mb outflow centered near 10° N, 130° E with strong convergence over South America.

3.7 Precipitation

Precipitation is not a well-measured quantity, especially over the oceans, yet it is the result of links among the moisture, thermodynamics and dynamics. It is of particular importance for coupling issues and, because of its direct impact on society, it is a crucial variable in studies of climate change. Significant differences exist between the Legates and Wilmott (1990) estimates of tropical precipitation and climatologies derived from satellite measurements of outgoing longwave radiation (OLR) (e.g., Arkin and Ardanuy 1989). Given such

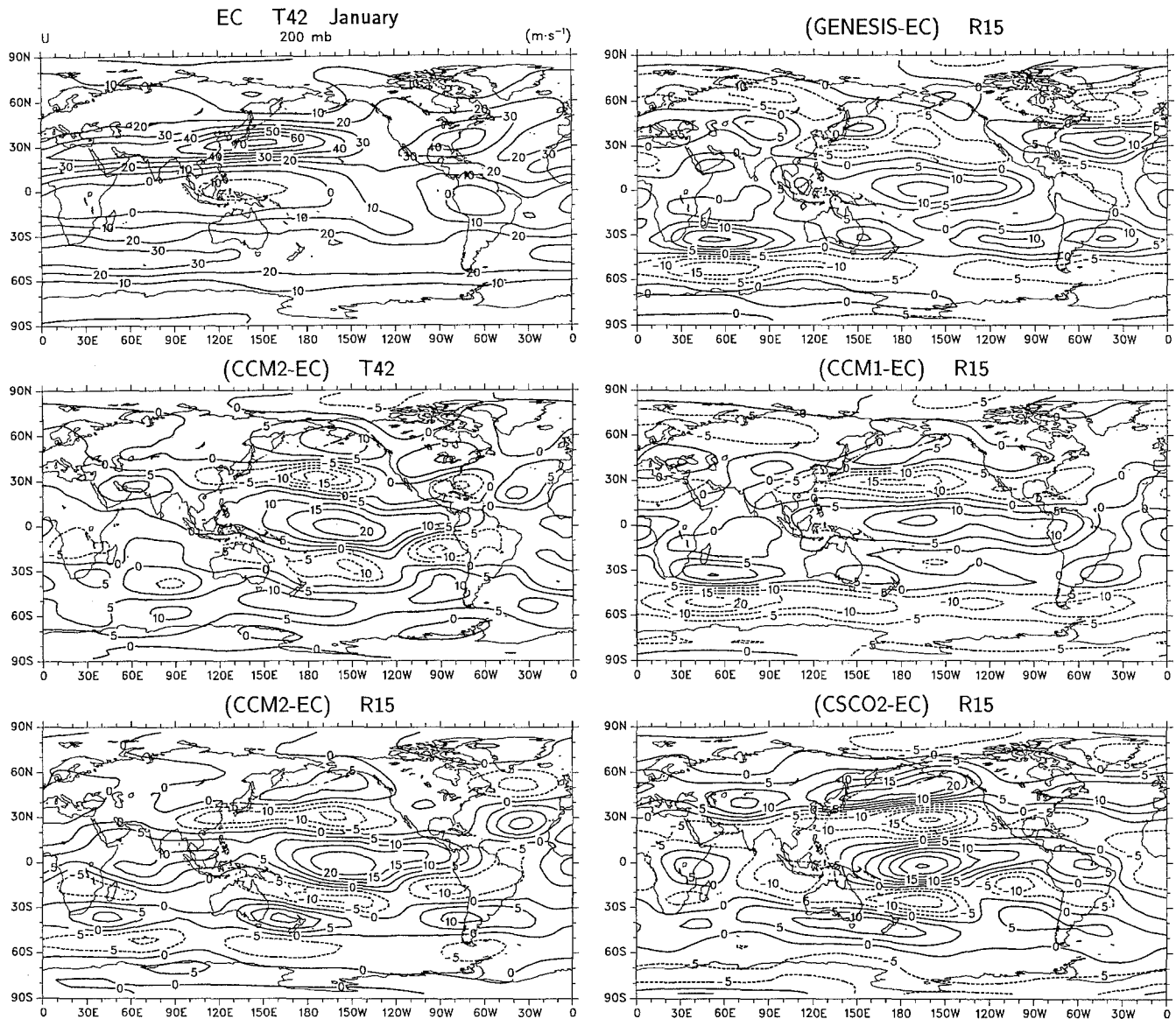


Fig. 9. Mean January zonal wind (m s^{-1}) at 200 mb from ECMWF, and differences from the ECMWF climatology for each CCM simulation. Differences are contoured in increments of 5 m s^{-1} and negative values are dashed

uncertainties in the observations, difference maps will not be presented; however, it is noteworthy that differences between observational estimates are mostly smaller than differences between observations and the CCM simulations.

Zonally-averaged profiles of total precipitation are shown in Fig. 15. The spike in the observations near 5°N in January results from a bullseye near 160°W of nearly 28 mm day^{-1} (see Fig. 16). This value is unrealistic and the existence of this maximum is highly questionable since no equivalent feature appears in satellite-derived or other precipitation climatologies. In January, CCM2 T42 has a zonal-mean maximum of nearly 9 mm day^{-1} near 10°S , which is larger than observed and is consistent with a stronger Hadley circulation (e.g., Fig. 13). Excessive localized precipitation at low latitudes during northern winter is a feature of the other CCM models as well, although less so for CCM1

(see also Fig. 16). CCM2 simulated precipitation agrees fairly well with observed minima in the subtropical high-pressure belts, and all CCM versions exceed observed values over NH middle latitudes and are lower than observed over the southern oceans [errors which are also common to most other AGCMs, independent of resolution (Boer et al. (1991))]. The latter region, in particular, has very few direct observations, so differences there are more uncertain. GENESIS overestimates precipitation at nearly all latitudes.

All CCM simulated precipitation distributions during July exceed the estimates of Legates and Willmott at nearly all latitudes, especially in the SH middle latitudes where the models place a maximum near 40°S (Fig. 15). Tropical precipitation rates are larger than observed in CCM2 and GENESIS with maxima slightly further north than in the climatology, while CSCO2 and CCM1 zonally-averaged rates are smaller than val-

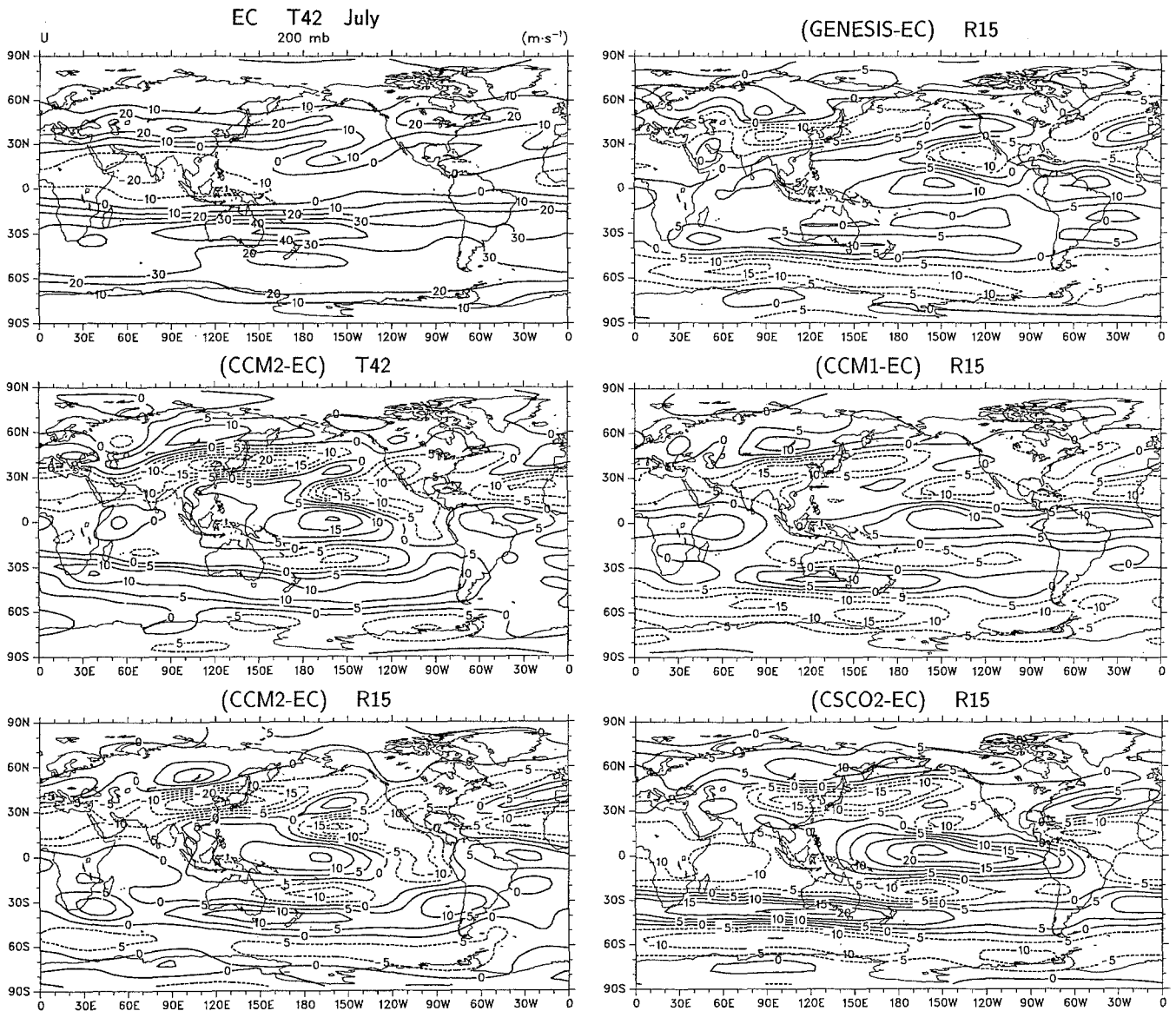


Fig. 10. As in Fig. 9, but for July

ues from the observed climatology by roughly 2 mm day^{-1} .

Area-averaged precipitation rates are presented in Table 2 for the globe (90° S to 90° N), the NH extratropics (20° N to 90° N), the SH extratropics (90° S to 20° S), and the tropics (20° S to 20° N). On such large spatial scales, the precipitation rates from the various versions of the CCM are generally within 10% of each other and the Legates and Wilmott climatology. The exception is the GENESIS model from which precipitation rates are about 30% larger than any of the other models. This has been found to be primarily due to an overly large value of prescribed ocean roughness length in GENESIS (Pollard, personal communication).

The local distributions of precipitation are shown in Figs. 16 and 17. The tendency for excessive precipitation in January over the monsoon regions and regions of high topography is evident in each CCM version,

which is consistent with the erroneously strong divergent outflow centers noted in Fig. 13. These biases are especially evident in CCM2 and perhaps, to a lesser extent, in GENESIS. In particular, CCM2 T42 has a local precipitation maximum of 36 mm day^{-1} over New Guinea in January, and CCM2 R15 has a maximum in excess of 24 mm day^{-1} . This localized positioning and erroneous intensity of the deep convection in the western Pacific apparently negative affect (through anomalous latent heating) the CCM2 stationary waves and appear to contribute to the reverse PNA teleconnection pattern and the misplacement of the Aleutian low (Fig. 7) and the ridge over the west coast of North America (Fig. 11) (see Hoerling et al. 1993). Precipitation rates in CCM1 are smaller than in the other versions and agree better with the climatological estimates, which may account for the generally smaller errors in the rotational and divergent wind components noted earlier.

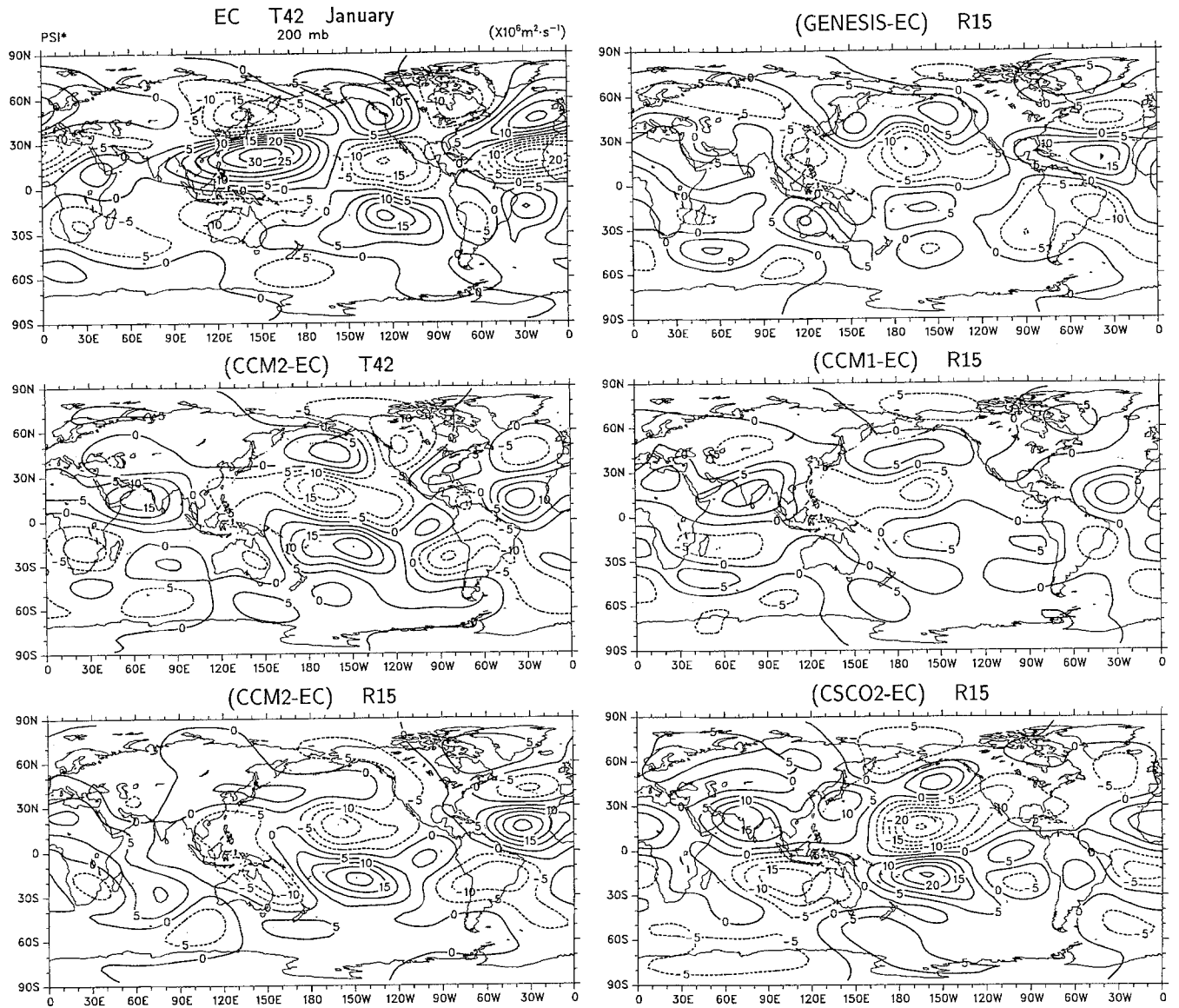


Fig. 11. Mean January eddy streamfunction ($10^6 \text{ m}^2 \text{ s}^{-1}$) at 200 mb from ECMWF, and differences from the ECMWF climatology for each CCM simulation. Differences are contoured in increments of $5 \times 10^6 \text{ m}^2 \text{ s}^{-1}$ and negative values are dashed

Simulated July rainfall rates show considerable local variability among models and with observations (Fig. 17). The observed zonally-elongated precipitation over the eastern tropical Pacific just north of the equator is in good agreement with measurements of OLR and is associated with the Intertropical Convergence Zone (ITCZ). This feature is generally not well simulated in the CCM versions. Precipitation rates over the summer monsoon regions are too strong in the CCM versions, and each model except GENESIS simulates a horse-shoe-shaped pattern that is not observed, with maxima over the Arabian Sea and southern Tibetan plateau and a minimum over much of central India. This same pattern was also noted in a recent Monsoon Numerical Experimentation Working Group (MONEG) study of the simulation of interannual variability of monsoon activity in a large number of AGCMs (WMO 1992). Presumably, this pattern in the CCM versions is re-

lated to the strong surface convergence noted in the models over southern India and the Arabian Sea (not shown) and the orographic effect of the Himalayas to the north. Over Central America, excessive precipitation is notable in CCM2 and GENESIS, reaching a maximum value of 36 mm day^{-1} in CCM2, that is consistent with the very strong upper-level outflow noted in Fig. 14.

3.8 Clouds and radiation

The definition of a cloud may differ from model to model and between a model and observations, especially when comparing specific cloud types (e.g., low, middle, high, stratus, or convective clouds). Total cloud cover is perhaps more comparable, and area-av-

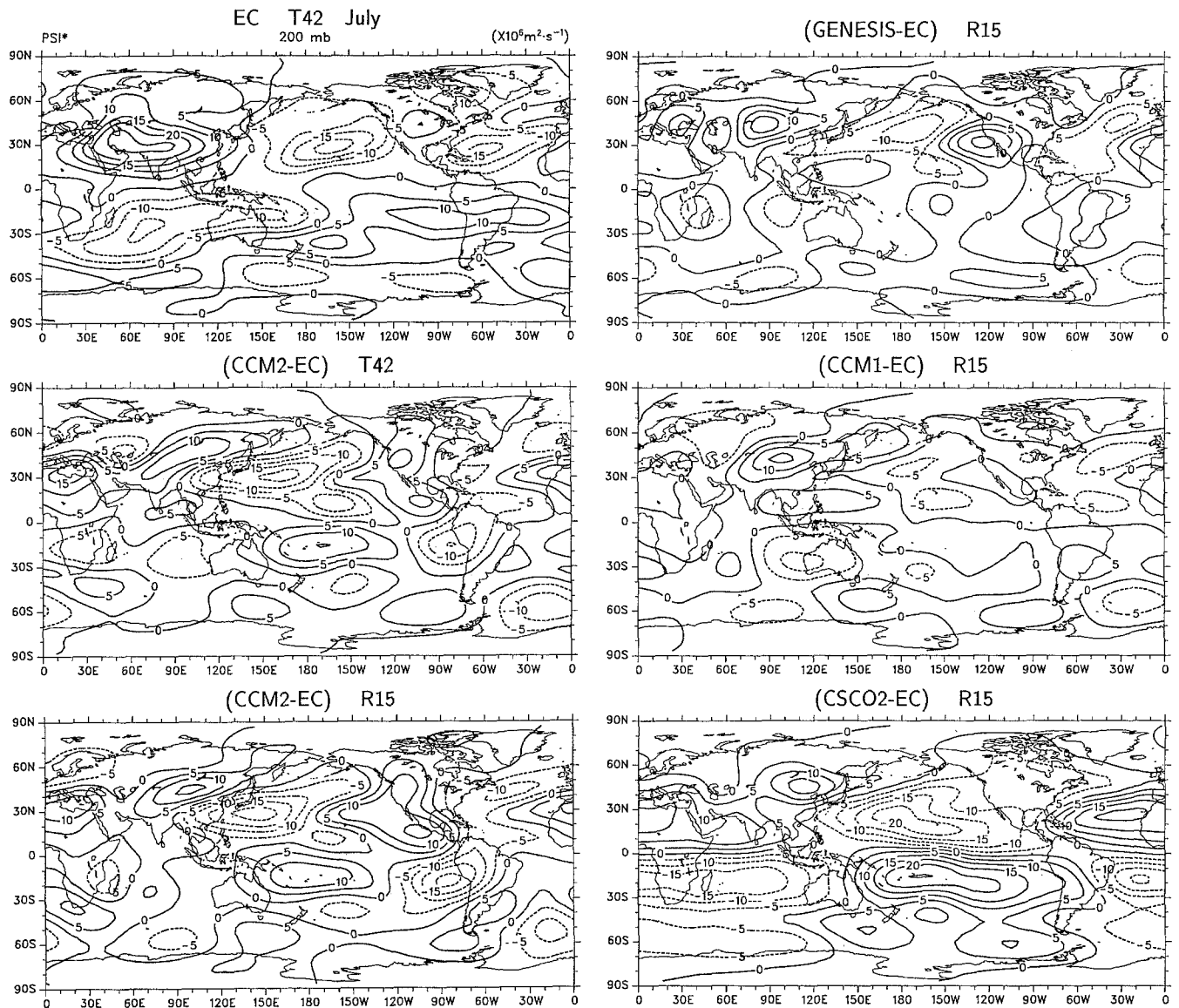


Fig. 12. As in Fig. 11, but for July

eraged total cloud amount from ISCCP and the CCM seasonal-cycle integrations can be compared in Table 3.

Globally-averaged estimates of total cloud from ISCCP data are near 62% for both January and July, which closely agree with estimates from the ground-based climatology of Warren et al. (1986, 1988) and are about 9% higher than seasonal values from Nimbus-7 Cloud Matrix data. Rossow et al. (1993) report that the global annual mean cloud amount from ISCCP has varied by about 4% on a time scale of 2 to 4 years over the 8-year data record. Globally-averaged cloud cover from the CCM simulations generally falls within the observational range. CCM1, CCM2 and CSCO2 total cloud amounts are lower than the ISCCP climatology, with CCM1 having the least cloud (47.4% in January and 47.8% in July), while GENESIS simulated total cloud cover is close to the ISCCP climatology. Regional maps (not shown) indicate that the largest differ-

ences from ISCCP in all CCM version occur in the SH middle latitudes during both January and July and over NH middle latitudes in July where simulated cloud amounts are lower than ISCCP values. These differences are most pronounced in CCM1 where total cloud cover is below ISCCP values by up to 45% locally over the middle latitude oceans of the summer hemisphere. All CCM versions also underestimate total cloudiness in the stratus regimes over the subtropical eastern oceans. GENESIS total cloud amounts are generally higher than ISCCP values over tropical oceans.

Given the uncertainty in the definition of clouds, however, it is easier and perhaps better to compare measurable radiative quantities. The earth's radiation balance constitutes the net forcing of the climate system, and it critically depends on many mechanisms that are internal to the system, for instance the hydrological cycle. Therefore, the ability of a model to correctly si-

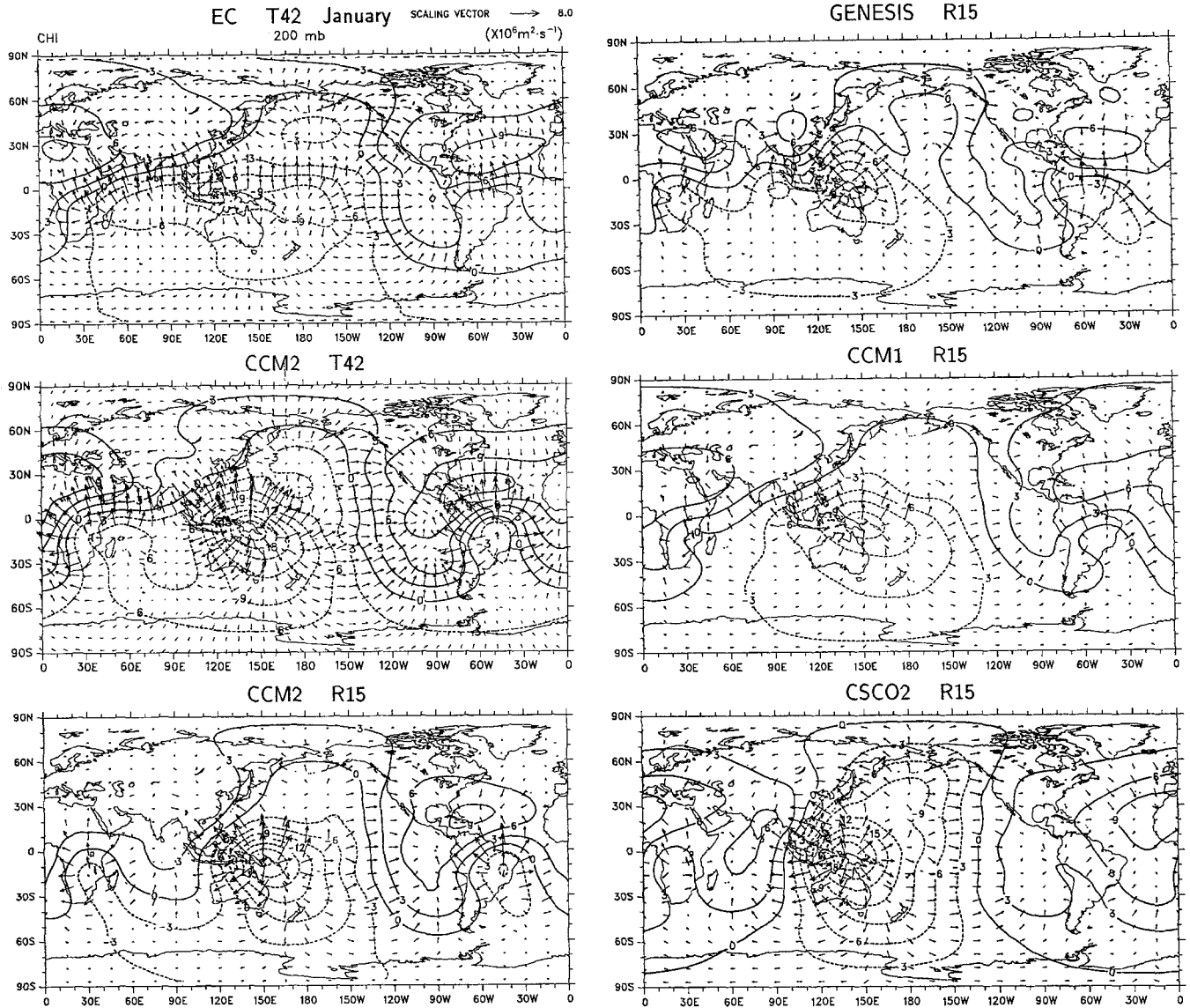


Fig. 13. Mean January velocity potential ($10^6 \text{ m}^2 \text{ s}^{-1}$) and vector divergent wind at 200 mb from ECMWF and each CCM simulation. The contour increment is $3 \times 10^6 \text{ m}^2 \text{ s}^{-1}$ and negative values

are dashed. The scaling vector of the divergent wind is 8 m s^{-1} and is given at the top of the figure

simulate this balance is a measure of much more than the radiative transfer algorithms employed.

In the tropics, low values of OLR are often used to indicate the presence of cold, high cloud tops associated with deep convection and precipitation. Spatially-averaged values of OLR are summarized in Table 4 for the ERBE observations and the CCM simulated values. Systematic differences in OLR can be seen in these numbers, most notably in the tropics where the GENESIS and CCM1 models exhibit biases around $+14 \text{ W m}^{-2}$, while the CSCO2 model exhibits a bias around -15 W m^{-2} . Biases are generally smallest in CCM2, although the NH summer warm bias in middle and high latitudes of CCM2 is manifested as OLR values nearly 20 W m^{-2} larger than ERBE values.

The global spatial distribution of differences from ERBE measurements of OLR are shown in Figs. 18 and 19. In the tropics and subtropics, the negative bias

of CSCO2 is pronounced nearly everywhere, with regional differences as large as -45 W m^{-2} in July. Equally large errors are seen in the other CCM versions as well, but they are generally not as geographically extensive. Neither GENESIS nor CCM1 fully captures the minima in OLR associated with the ITCZ and the monsoon circulations in either season, whereas the largest biases in CCM2 OLR are related to the centralized positioning of the deep convection over New Guinea in January and Central America in July and the warm bias over the NH during summer. In general, the CCM OLR biases evident in the tropics and subtropics are consistent with regional errors noted in the simulated irrotational flow and precipitation fields, which are not as well measured as OLR.

Spatially-averaged values of the solar radiation absorbed by the earth-atmosphere system are summarized in Table 5 for the ERBE observations and the

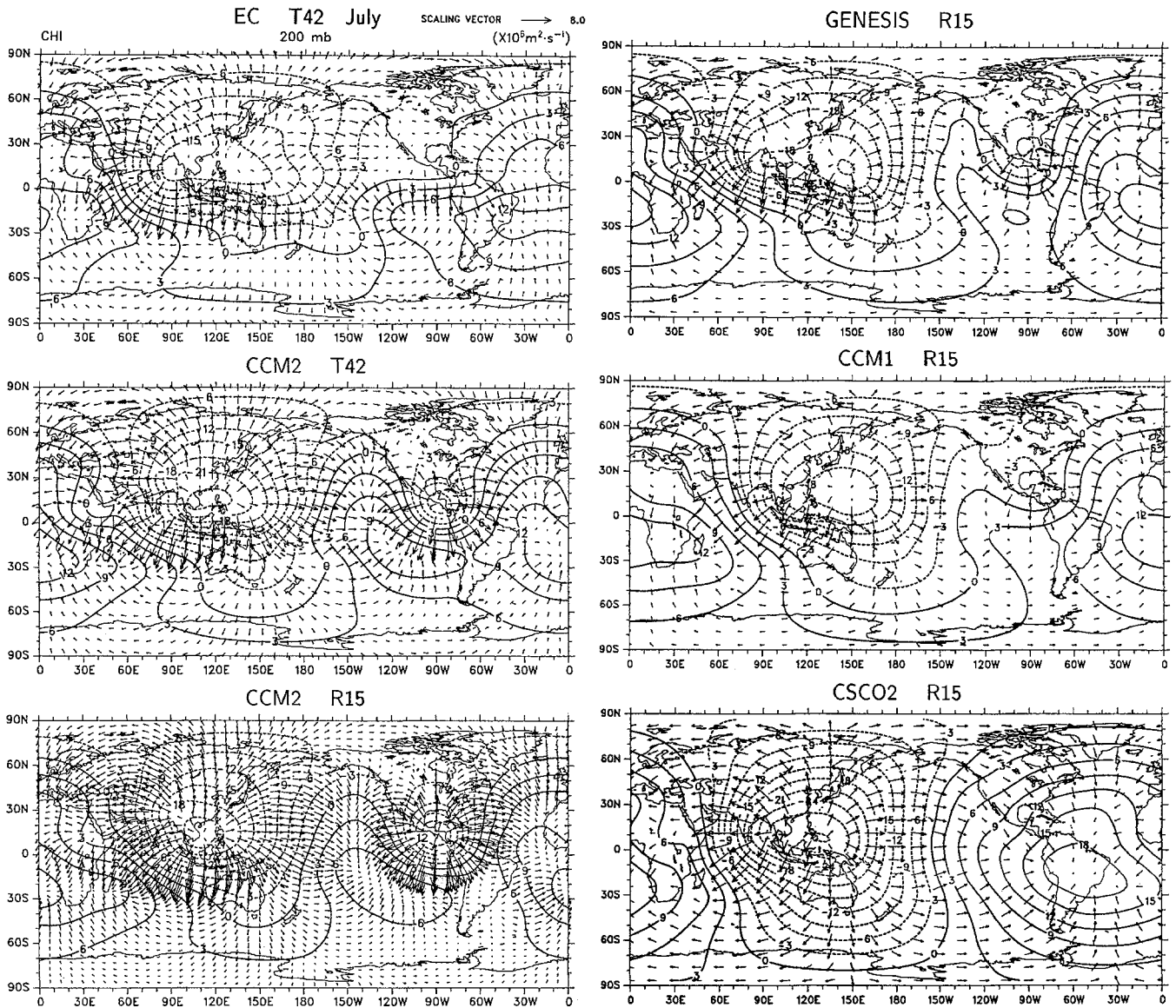


Fig. 14. As in Fig. 13, but for July

CCM simulated values. As for the case of OLR, systematic differences are evident in these numbers. Generally, on a global scale the CCM1, GENESIS, and CCM2 models exhibit similar radiative characteristics (a $+5 \text{ W m}^{-2}$ to $+11 \text{ W m}^{-2}$ bias) while the CSC02 model exhibits a -4 W m^{-2} to -8 W m^{-2} bias. As before, the tropical radiative characteristics differentiate the various models the most, where the GENESIS model exhibits a $+8 \text{ W m}^{-2}$ bias in January and the CSC02 model exhibits a year-round bias of approximately -17 W m^{-2} . Errors common to all CCM versions are that too much solar radiation is absorbed in the middle latitudes of the summer hemisphere (Table 5) and locally in the subtropical eastern oceans in the stratus regimes (not shown), and these biases correspond well to biases in total cloud amount. The middle latitude biases are most pronounced in a zonal-mean sense in CCM2 during July, and they are consistent with the thermal biases noted earlier.

4 Discussion

Climate system models are needed to understand and consider simultaneously the wide range of complex interacting physical, chemical and biological processes that characterize the atmosphere, ocean and land. Before simulations from such models can be fully comprehended, it is necessary to understand the strengths and weaknesses of the component models. Atmospheric modeling at NCAR has a long history and the CCM has been an invaluable contribution to climate research for over a decade. Although various versions have been extensively used in the research community and work continues with these different models, no extensive comparison of the CCM family of models exists. This study summarizes a more comprehensive comparison given in Hurrell et al. (1993). Four CCM versions were examined, including two standard CCM versions, CCM1 and CCM2, and two widely cited re-

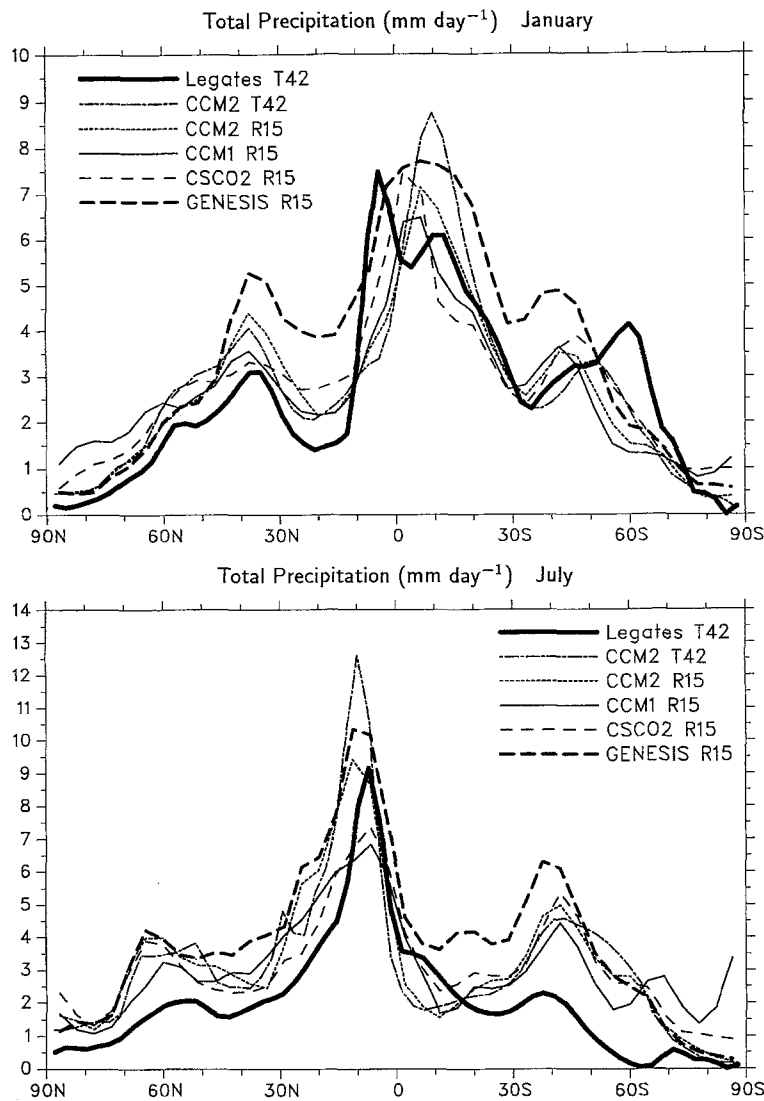


Fig. 15. Zonally-averaged mean total precipitation (mm day^{-1}) for January (*top*) and July (*bottom*)

search versions, CSCO2 and GENESIS. A documentation of the strengths and weaknesses of each CCM version can illustrate evolutionary improvements as well as common biases and errors. The latter are especially important to note before using the CCM in a coupled interactive sense.

Implicit in the results of this study is information on the effects of differences in the numerical schemes, horizontal and vertical resolutions, and physical parameterizations employed by the different CCM versions (e.g., Table 1). It is difficult to relate particular model biases to specific differences in model formulations without conducting carefully planned sensitivity experiments, and even then nonlinearities in the model can make results difficult to interpret. Nonetheless, an interpretation of some of the main differences in the simulated CCM climates is worthwhile, speculative though it may be.

The parameterization of moist convection differs considerably among the different CCM versions. Early versions of the CCM (CCM0 and CCM1) used a simple moist convective adjustment procedure (Manabe et al.

1965) that ignores the complexities of the physical processes that occur in the real atmosphere. The temperatures simulated by CCM0, for example, are $5\text{--}8^\circ\text{C}$ lower than observed in the tropical upper troposphere, and the simulated water vapor mixing ratios exhibit a correspondingly large dry bias (e.g., Pitcher et al. 1983). Biases of similar magnitudes remain in CCM1 (Figs. 1–3). Albrecht et al. (1986) show that the inclusion of explicit penetrative eddy fluxes of heat and moisture into CCM0 largely alleviates the biases in simulated temperature and moisture, and several other aspects of the simulated circulation are significantly improved (Meehl and Albrecht 1988). The cumulus parameterization scheme of Albrecht et al. (1986) is included in CSCO2; however, the excessively warm and moist upper tropical troposphere in CSCO2 (Figs. 1–3) suggests that changes made to other parameterizations have had an effect, for example through modifications made to the cloud and radiation scheme of Ramanathan et al. (1983) (see Washington and Meehl 1993).

The NCAR CCM2 represents an entirely new AGCM for which most aspects of the CCM1 model

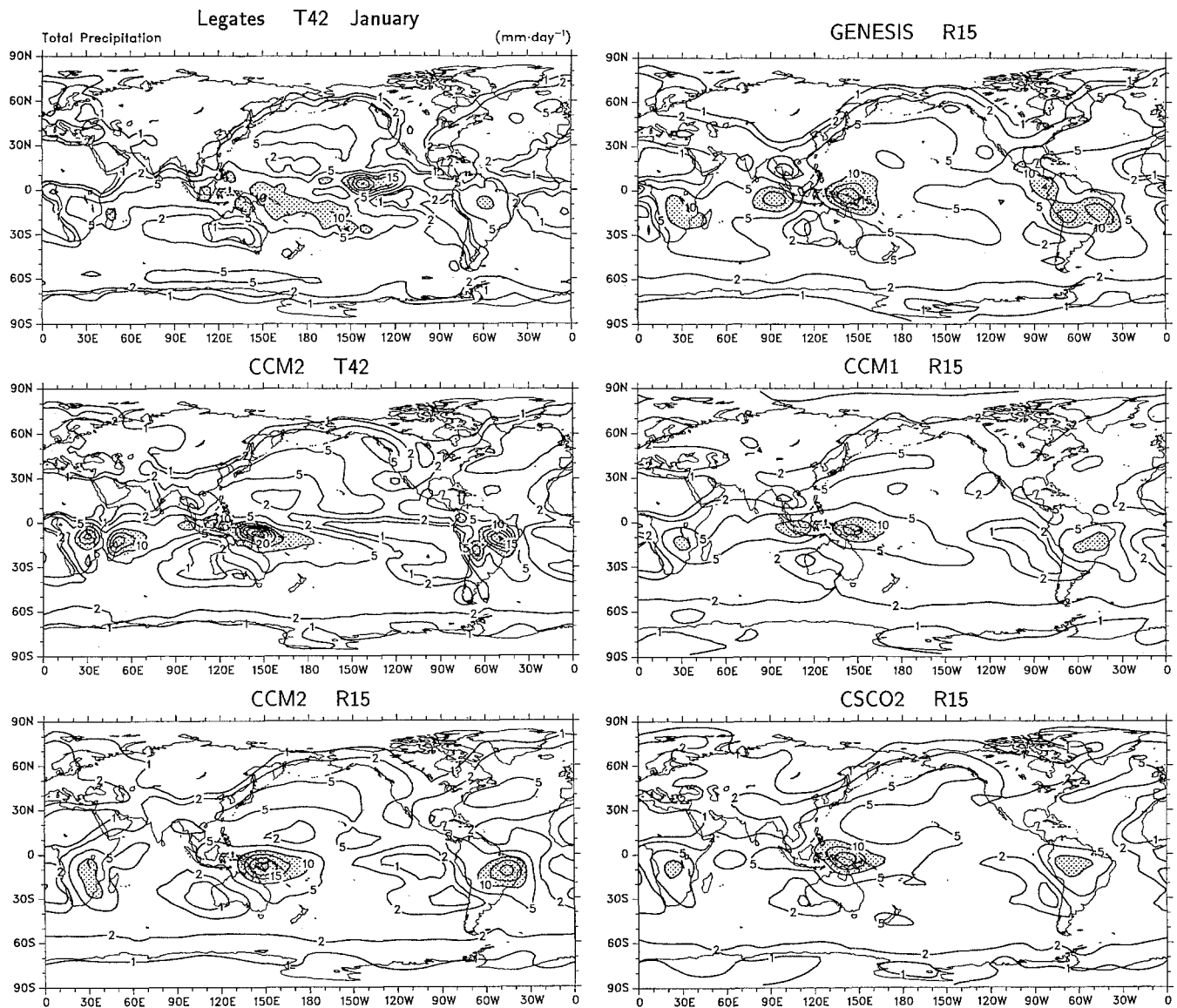


Fig. 16. Mean January total precipitation (mm day^{-1}) from Legates and Wilmott (1990) and each CCM simulation. The contour increment is 5 mm day^{-1} , except the 1 and 2 mm day^{-1} contours are included. Values greater than 10 mm day^{-1} are shaded

Table 2. Area-averaged precipitation rates (mm day^{-1})

	Global ($90^\circ \text{ S} - 90^\circ \text{ N}$)	NH extratropics ($20^\circ \text{ N} - 90^\circ \text{ N}$)	SH extratropics ($90^\circ \text{ S} - 20^\circ \text{ S}$)	Tropics ($20^\circ \text{ S} - 20^\circ \text{ N}$)
January				
Legates T42	3.3	1.9	3.0	4.9
CCM2 T42	3.5	2.6	2.7	5.2
CCM2 R15	3.4	2.8	2.5	4.6
GENESIS	4.5	3.4	3.6	6.2
CCM1	3.2	2.6	2.5	4.3
CSCO2	3.5	2.7	2.7	4.7
July				
Legates T42	2.7	2.1	1.3	4.8
CCM2 T42	3.8	3.5	3.0	5.0
CCM2 R15	3.8	3.5	3.1	4.6
GENESIS	4.8	4.1	3.9	6.1
CCM1	3.5	3.3	2.9	4.1
CSCO2	3.6	3.0	3.2	4.5

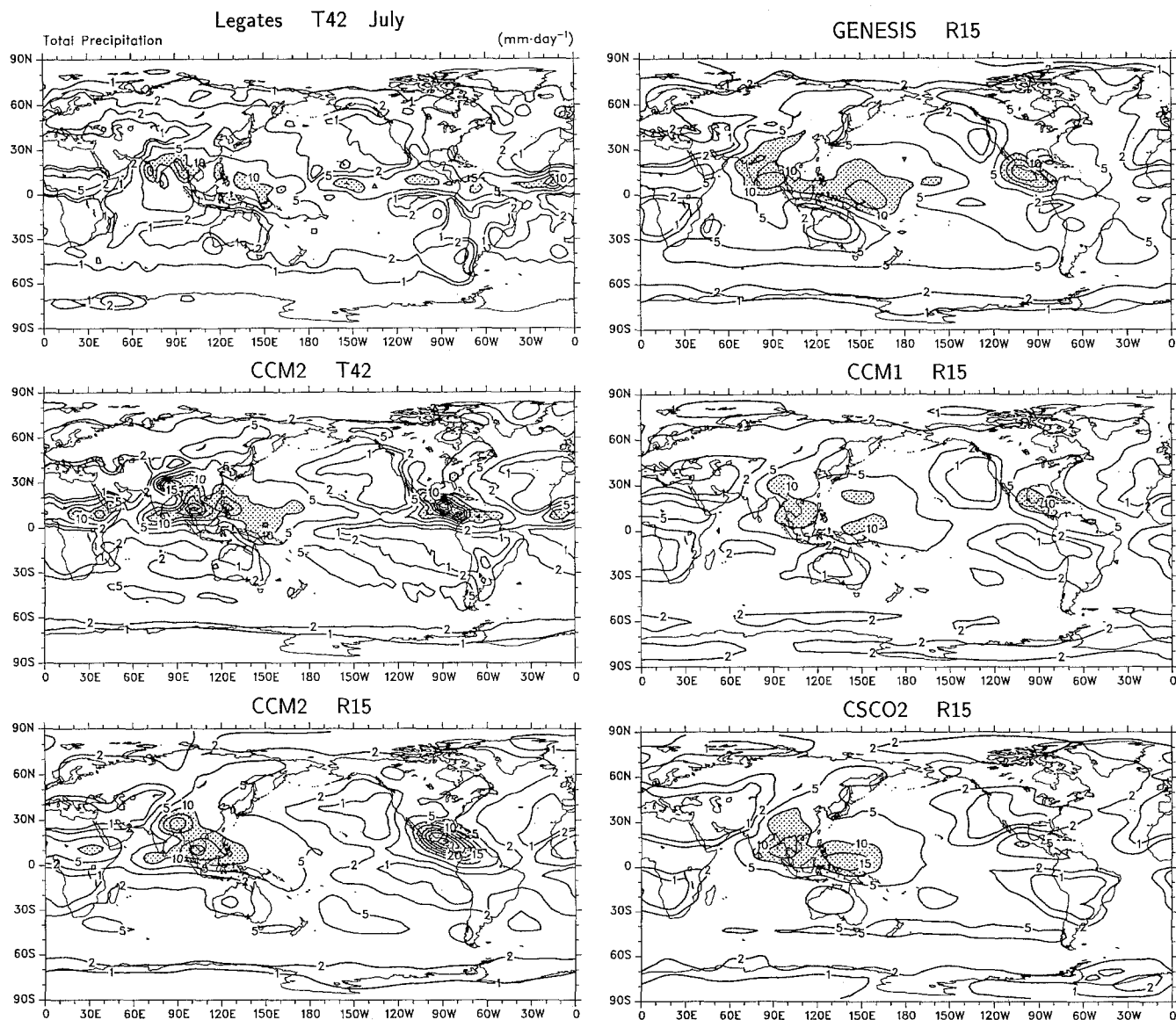


Fig. 17. As in Fig. 16, but for July

Table 3. Area-averaged total cloud amount (%). Values for CCM1 and CSCO2 differ from those presented in Hurrell et al. (1993) due to the correction of a processing error

	Global (90° S–90° N)	NH extratropics (20° N–90° N)	SH extratropics (90° S–20° S)	Tropics (20° S–20° N)
January				
ISCCP T42	62.0	58.0	67.7	60.2
CCM2 T42	54.6	55.6	51.9	56.2
CCM2 R15	58.1	58.9	54.0	60.8
GENESIS	61.9	55.4	69.9	60.8
CCM1	47.4	46.8	44.0	50.8
CSCO2	51.3	48.4	50.3	54.5
July				
ISCCP T42	62.4	58.7	68.9	59.7
CCM2 T42	50.6	45.0	54.6	52.1
CCM2 R15	54.4	48.1	56.8	57.6
GENESIS	60.8	54.3	65.8	61.9
CCM1	47.8	43.5	53.2	47.8
CSCO2	51.2	43.5	57.8	52.1

Table 4. Area-averaged OLR (W m^{-2})

	Global (90° S–90° N)	NH extratropics (20° N–90° N)	SH extratropics (90° S–20° S)	Tropics (20° S–20° N)
January				
ERBE T42	233.3	212.8	236.4	250.5
CCM2 T42	236.9	215.4	239.6	255.7
CCM2 R15	232.9	212.7	235.6	247.4
GENESIS	239.3	216.9	231.7	263.9
CCM1	240.6	214.4	237.6	264.7
CSCO2	222.6	201.4	228.7	235.0
July				
ERBE T42	239.2	249.7	214.0	253.8
CCM2 T42	247.8	267.3	215.7	260.3
CCM2 R15	244.4	266.3	212.9	252.4
GENESIS	246.7	257.3	212.4	266.0
CCM1	246.8	254.6	213.9	267.4
CSCO2	227.7	244.1	198.4	238.4

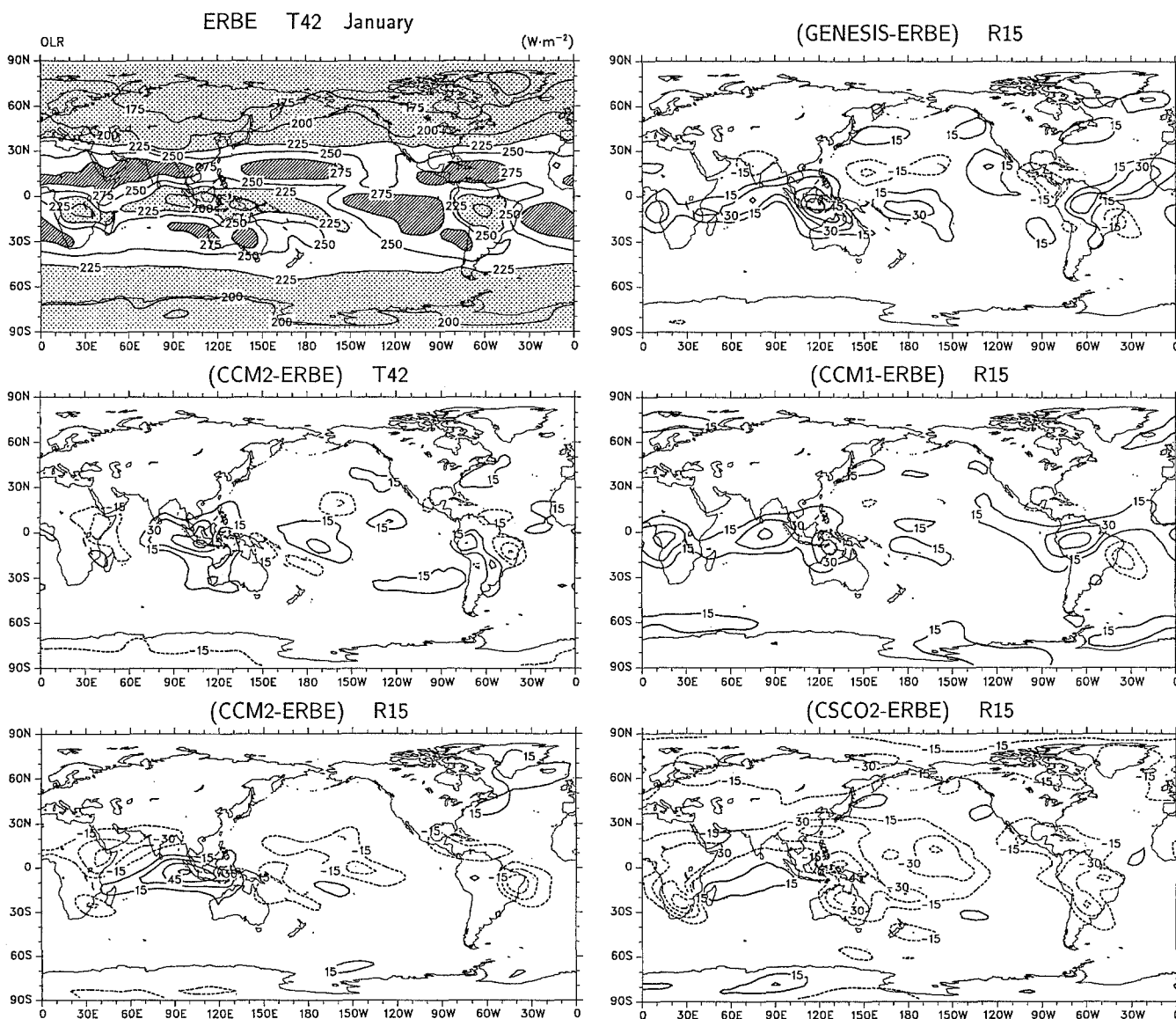


Fig. 18. Mean January OLR (W m^{-2}) from ERBE, and differences from the ERBE climatology for each CCM simulation. The ERBE values are contoured every 25 W m^{-2} , with values greater than 275 W m^{-2} hatched and values less than 225 W m^{-2} shaded.

Differences are contoured in increments of 15 W m^{-2} , negative values are dashed, and the zero contour has been suppressed for clarity

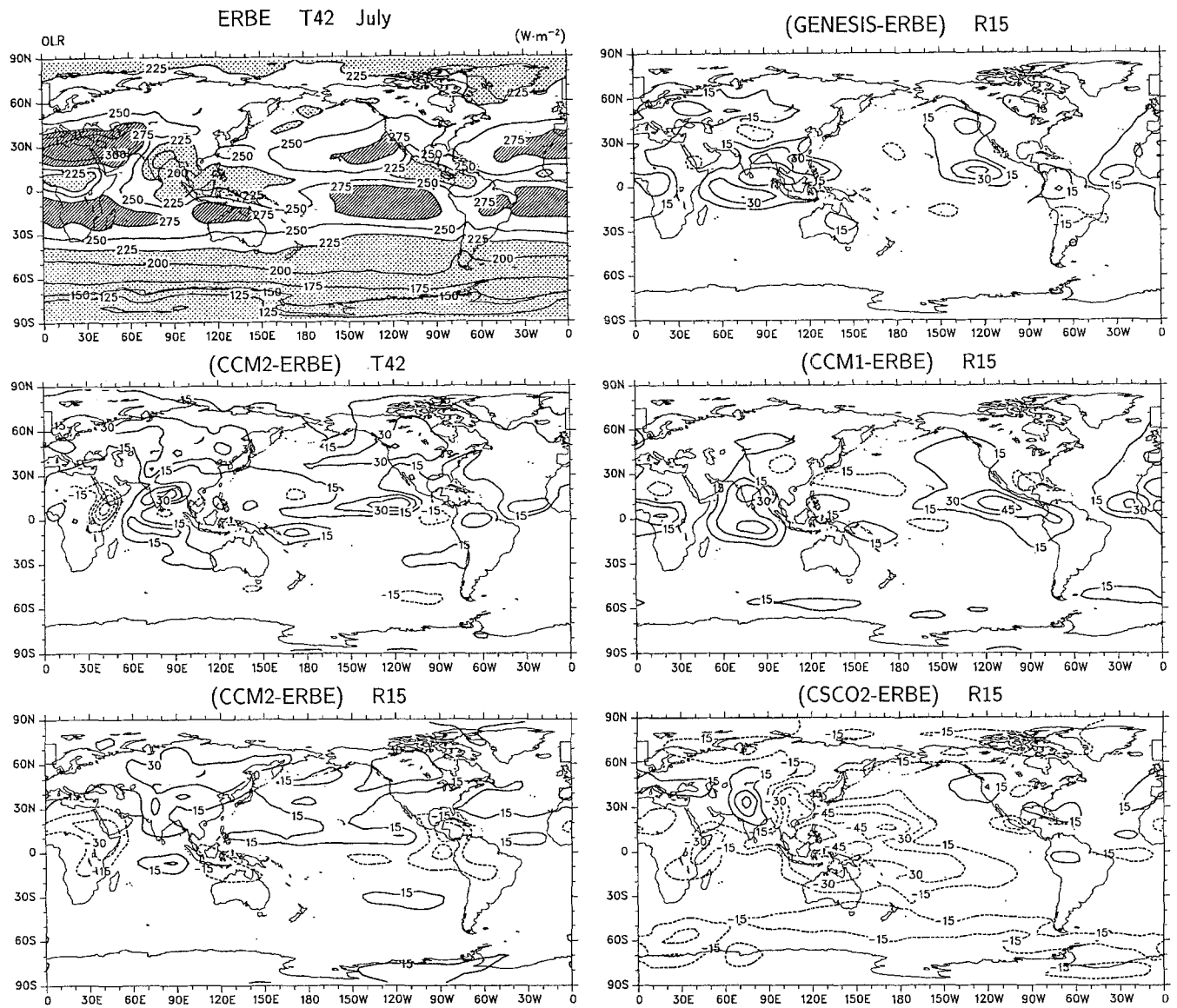


Fig. 19. As in Fig. 18, but for July

Table 5. Area-averaged absorbed solar radiation (W m^{-2})

	Global (90° S–90° N)	NH extratropics (20° N–90° N)	SH extratropics (90° S–20° S)	Tropics (20° S–20° N)
January				
ERBE T42	247.3	105.5	321.5	314.7
CCM2 T42	256.1	108.8	341.6	317.6
CCM2 R15	258.0	105.3	338.2	317.7
GENESIS	254.8	101.8	325.7	322.3
CCM1	254.7	99.8	339.6	312.2
CSCO2	243.8	95.4	325.2	298.9
July				
ERBE T42	233.6	316.4	95.5	288.7
CCM2 T42	244.1	344.8	97.6	289.8
CCM2 R15	240.7	344.2	86.2	282.6
GENESIS	238.6	337.1	80.9	287.1
CCM1	232.7	325.7	80.6	281.3
CSCO2	225.0	319.0	75.2	270.9

formulation have been either extensively modified or replaced (Hack et al. 1993). A major change that had a positive impact on the CCM2 climate was the incorporation of a semi-Lagrangian transport (SLT) scheme for advecting water vapor. Williamson and Rasch (1994), for example, show that the CCM2 has higher specific humidity in the troposphere compared to a version integrated with the spectral advection approach used in earlier CCM versions. Presumably, the SLT scheme used in GENESIS has a similar positive effect. Another change made to the CCM2 formulation is the inclusion of a simple mass flux scheme developed by Hack (1994) that represents all types of moist convection. Hack (1994) contrasts the mean control climate produced by the CCM2 with the climate simulated using a conventional moist adiabatic adjustment procedure. He shows that the new mass flux representation of moist convective processes significantly moistens and warms the CCM2 troposphere at all latitudes but particularly in the tropics. Moreover, such changes apparently contribute to differences in the general structure and magnitude of the simulated precipitation field. The overall weaker and broader precipitation features of the simulation with moist adiabatic adjustment in CCM2 roughly parallel the differences between CCM1 and CCM2 simulated precipitation seen in Figs. 15–17 and Table 2.

Differences in precipitation between the CCM versions, however, likely cannot be explained through differences in convective schemes alone. Other factors are important such as the parameterization of the atmospheric boundary layer and differences in orography, vegetation, soil moisture and cloudiness. A recent paper by Fennessy et al. (1994) shows the sensitivity of the simulated Indian monsoon to the specification of orography in an AGCM. Meehl (1994) demonstrates the sensitivity of the Indian monsoon circulations of various AGCMs, including versions of CCM0 and CCM1, to land-sea temperature contrasts in the models, and he further explores the contributions to those contrasts by external conditions related to surface albedo and internal feedbacks involving soil moisture. For the experimental results presented in this paper, the land surface properties of CCM1 and CCM2 are specified (but differ between the models), while GENESIS employs the land surface transfer model of Pollard and Thompson (1994) and CSCO2 makes use of model-derived rates of precipitation, evaporation and sublimation to simulate changes in soil moisture and snow cover (see Washington and VerPlank 1986).

Biases in CCM2 simulated precipitation have been shown to be sensitive to additional factors as well. In particular, two factors which appear important are the diagnosis of cloud optical properties (JJ Hack and JT Kiehl 1994, manuscript in preparation) and the interaction between moist convection and the atmospheric boundary layer (which appears to have excessive water-vapor transport in deep convective regions, Hack 1994). Hack et al. (1994) report that the incorporation of improved cloud diagnostics into CCM2 moves the maximum diabatic heating in the western Pacific north-

ward, improves the Australian monsoon circulation, and results in a more realistic tropospheric stationary wave pattern across the North Pacific and North America (e.g., Fig. 11). The magnitude of the simulated precipitation (Fig. 16) remains unrealistically large, however, and the cause of this error is currently being studied.

Improvements in the cloud optical properties of CCM2 have also had a large impact on the radiative budget of the model. Use of a different effective drop size over continents and oceans significantly reduces the amount of absorbed solar radiation in middle latitudes of the NH during summer (Table 5), which in turn reduces the warm and moist biases (Figs. 2 and 3) as well as the bias in OLR evident in Fig. 19 (see Kiehl 1994). The inclusion in CCM2 of a diagnostic approach to specify the cloud liquid-water path as a function of the atmospheric state (JJ Hack and JT Kiehl 1994, manuscript in preparation) appears to further reduce the radiative and thermodynamic biases in the summer hemispheres. Moreover, these improvements do not appear to affect adversely other aspects of the CCM2 simulated climate. Differences between the radiation and cloud parameterizations of the different CCM versions are substantial (Table 1). The radiation budget of CCM0 is described in detail by Ramanathan et al. (1983), Smith and Vonder Haar (1991) and Kiehl and Ramanathan (1990) describe the radiation budget of R15 and T42 versions of CCM1, and Kiehl et al. (1994) describe the earth radiation budget simulation of CCM2.

Another aspect that complicates the interpretation of some of the results presented in this paper is that the CCM integrations were performed with climatological SSTs. A clear impact of this can be seen in maps of the simulated and observed interannual variability of numerous quantities (Hurrell et al. 1993). The influence of this lower boundary constraint on the mean fields is less clear, however. The localized nature of the precipitation maxima and divergence centers in the CCM simulated tropics may be due in part to the absence of interannually varying SSTs which zonally extend the heating and divergence patterns, for example in El Niño/Southern Oscillation events. Changes in the distribution of tropical heating can then influence extratropical circulations through teleconnections. Consider the significant CCM biases observed in the SLP (as well as the temperature and low-level winds) over the North Pacific. In CCM2 and CSCO2, these biases are related to a simulated Aleutian low that is weaker and farther west than observed in both models (Fig. 7). Trenberth (1990) and Trenberth and Hurrell (1994) have recently demonstrated that a substantial low-frequency change in the North Pacific atmosphere and ocean began in the late 1970s, and this change was manifested in the atmospheric circulation as a deeper and eastward shifted Aleutian low pressure center. Moreover, it appears as though this change is related to warmer tropical SSTs during the late 1970s and 1980s compared with previous decades. It is possible, therefore, that some aspects of the poor CCM simula-

tions of the Aleutian low are, at least partially, the result of the climatological SSTs used as a lower boundary condition in the model runs.

While it is not possible to answer such questions completely, some insight was gained for CCM2 by examining the mean results from an AMIP simulation. In this case, the CCM2 was integrated at T42 resolution using observed SSTs over the period January 1979 through December 1988. The results of the AMIP integration did show some small reduction in biases, such as a slightly more elongated region of precipitation and upper-tropospheric outflow over the western and central Pacific in January and about a 20% reduction of the westerly wind error over the central Pacific. However, all of the primary biases identified in this study and Hurrell et al. (1993) were still present in the AMIP simulation. It does appear, therefore, that the influence of observed SSTs on the largest biases noted in the CCM mean fields is small.

Comparison studies are only one approach to improve our understanding of the way models and the climate system behave. Given the enormous complexity of atmospheric general circulation models, the simple identification of differences from observations does not easily translate into model improvements. Moreover, many other important aspects of the ability of the CCM to simulate the observed climate were not presented in this study nor in the more complete work of Hurrell et al. (1993). Examples include the ability of the CCM to simulate observed variability on a wide array of time scales, or a more in-depth diagnosis of the CCM's simulated heat, momentum and water budgets. The results presented here are brief and only touch on the more obvious features and biases of the simulations. In this sense, the work of Hurrell et al. (1993) represents an atlas of the climate features of the different CCM versions that perhaps can be useful for evaluating the suitability of the models for many different applications.

Acknowledgements. This study is a summary of a more complete comparison that is available as an NCAR Technical Note (Hurrell et al. 1993). There are many people at NCAR that contributed to the overall project. I would especially like to thank Dr. James Hack and Mr. David Baumhefner for their help in compiling some of the material, and Dr. Gerald Meehl, Dr. David Polard and the Climate Modeling Section for providing the model data. I would also like to thank Dr. Kevin Trenberth for his advice and guidance and his useful comments on the manuscript. Ronna Bailey helped to prepare the tables, and Christian Guillemot helped with many of the figures.

References

- Albrecht BA, Ramanathan V, Boville BA (1986) The effects of cumulus heat and moisture transports on the simulation of climate with a general circulation model. *J Atmos Sci* 43:2443–2462
- Alexander RC, Mobly RL (1976) Monthly average sea-surface temperatures and ice-pack limits on a 1° global grid. *Mon Weather Rev* 104:143–148
- Arkin PA, Ardanuy PE (1989) Estimating climatic-scale precipitation from space: a review. *J Clim* 2:1229–1238
- Barkstrom BR, Harrison E, Smith G, Green R, Kibler J, Cess R, ERBE Science Team (1989) Earth Radiation Budget Experiment (ERBE) Archival and April 1985 results. *Bull Am Meteorol Soc* 70:1254–1262
- Boer GJ, Arpe K, Blackburn M, Déqué M, Gates WL, Hart TL, Le Treut H, Roeckner E, Sheinin DA, Simmonds I, Smith RNB, Tokioka T, Wetherald RT, Williamson D (1991) An intercomparison of the climates simulated by 14 atmospheric general circulation models. CAS/JSC Working Group on Numerical Experimentation WCRP-58 WMO/TD-No. 425 World Meteorological Organization, Geneva, Switzerland
- Boer GJ, Arpe K, Blackburn M, Déqué M, Gates WL, Hart TL, Le Treut H, Roeckner E, Sheinin DA, Simmonds I, Smith RNB, Tokioka T, Wetherald RT, Williamson D (1992) Some results from an intercomparison of the climates simulated by 14 atmospheric general circulation models. *J Geophys Res* 97:12771–12786
- Briegleb BP (1992) Delta-Eddington approximation for solar radiation in the NCAR Community Climate Model. *J. Geophys Res* 97:7603–7612
- Dorman CE, Bourke RH (1978) Precipitation over the Pacific Ocean, 30° S to 60° N. *Mon Weather Rev* 107:896–910
- ERBE Science Team (1986) First data from the Earth Radiation Budget Experiment (ERBE). *Bull Am Meteorol Soc* 67:818–824
- Fennessy MJ, Kinter III JL, Kirtman B, Marx L, Nigam S, Schneider E, Shukla J, Straus D, Vernekar A, Xue Y, Zhou J (1994) The simulated Indian monsoon: a GCM sensitivity study. *J Clim* 7:33–43
- Gates WL (1992) AMIP: The Atmospheric Model Intercomparison Project. *Bull Am Meteorol Soc* 73:1962–1970
- Gates WL, Rowntree PR, Zeng Q-C (1990) Validation of climate models. In: Houghton JT, Jenkins GJ, Ephraums JJ (eds) *Climate change, the IPCC scientific assessment*. Cambridge University Press, Cambridge, UK, pp 93–130
- Gates WL, Mitchell JFB, Boer GJ, Cubasch U, Meleshko VP (1992) Climate modeling, climate prediction and model validation. In: Houghton JT, Callander BA, Varney SK (eds) *Climate change 1992, the supplementary report to the IPCC scientific assessment*. Cambridge University Press, Cambridge, UK, pp 97–134
- Hack JJ (1994) Parameterization of moist convection in the NCAR Community Climate Model (CCM2). *J Geophys Res* 99:5551–5568
- Hack JJ, Boville BA, Briegleb BP, Kiehl JT, Rasch PJ, Williamson DL (1993) Description of the NCAR Community Climate Model (CCM2). NCAR Technical Note NCAR/TN-382 + STR National Center for Atmospheric Research Boulder Colorado
- Hack JJ, Boville BA, Kiehl JT, Rasch PJ, Williamson DL (1994) Climate statistics from the NCAR Community Climate Model (CCM2). *J Geophys Res* (in press)
- Hoerling MP, DeHaan LS, Hurrell JW (1993) Diagnosis and sensitivity of the wintertime 200 hPa circulation in NCAR community climate models. NCAR Technical Note NCAR/TN-394 + STR National Center for Atmospheric Research, Boulder, Colorado
- Hughes NA (1984) Global cloud climatologies: a historical review. *J Clim Appl Meteorol* 23:724–751
- Hurrell JW, Campbell GG (1992) Monthly mean global satellite data sets available in CCM history tape format. NCAR Technical Note NCAR/TN-371 + STR National Center for Atmospheric Research, Boulder, Colorado
- Hurrell JW, Hack JJ, Baumhefner DP (1993) Comparison of NCAR Community Climate Model (CCM) climates. NCAR Technical Note NCAR/TN-395 + STR National Center for Atmospheric Research, Boulder, Colorado
- Jaeger L (1983) Monthly and areal patterns of mean global precipitation. In: Street-Perrott A et al. (ed) *Variations in the global water budget*. D. Reidel, Dordrecht

- Kiehl JT (1994) Sensitivity of a GCM climate simulation to differences in continental versus marine cloud drop size. *J Geophys Res* (in press)
- Kiehl JT, Ramanathan V (1990) Comparison of cloud forcing derived from the earth radiation budget experiment with that simulated by the NCAR Community Climate Model. *J Geophys Res* 95:11679–11698
- Kiehl JT, Briegleb BP (1991) A new parameterization of the absorptance due to the 15 μm band system of carbon dioxide. *J Geophys Res* 96:9013–9019
- Kiehl JT, Briegleb BP (1992) Comparison of the observed and calculated clear sky greenhouse effect: implications for climate studies. *J Geophys Res* 97:10037–10049
- Kiehl JT, Wolski RJ, Briegleb BP, Ramanathan V (1987) Documentation of radiation and cloud routines in the NCAR Community Climate Model (CCM1). NCAR Technical Note NCAR/TN-288+IA National Center for Atmospheric Research, Boulder, Colorado
- Kiehl JT, Hack JJ, Briegleb BP (1994) The simulated earth radiation budget of the NCAR CCM2 and comparisons with the Earth Radiation Budget Experiment (ERBE). *J Geophys Res* (in press)
- Kreitzberg CW, Perkey DJ (1976) Release of potential instability: Part I. A sequential plume model within a hydrostatic primitive equation model. *J Atmos Sci* 33:456–475
- Legates DR, Willmott CJ (1990) Mean seasonal and spatial variability in gauge-corrected, global precipitation. *Int J Climatol* 10:111–128
- Manabe S, Smagorinsky J, Strickler RF (1965) Simulated climatology of a general circulation model with a hydrologic cycle. *Mon Weather Rev* 93:769–798
- Meehl GA (1994) Influence of the land surface in the Asian summer monsoon: external conditions versus internal feedbacks. *J Clim* 7:1033–1049
- Meehl GA, Albrecht BA (1988) Tropospheric temperatures and Southern Hemisphere circulation. *Mon Weather Rev* 116:953–960
- Pitcher EJ, Malone RC, Ramanathan V, Blackmon ML, Puri K, Bourke W (1983) January and July simulations with a spectral general circulation model. *J Atmos Sci* 40:580–604
- Pollard D, Thompson SL (1994) Use of a land surface transfer scheme (LSX) in a global climate model: the response to doubling stomatal resistance. *Glob Planet Change* (in press)
- Ramanathan V, Pitcher EJ, Malone RC, Blackmon ML (1983) The response of a spectral general circulation model to refinements in radiative processes. *J Atmos Sci* 40: 605–630
- Rossow WB, Schiffer RA (1991) ISCCP cloud data products. *Bull Am Meteorol Soc* 72:2–20
- Rossow WB, Garder LC (1993a) Cloud detection using satellite measurements of infrared and visible radiances for ISCCP. *J Clim* 6:2341–2369
- Rossow WB, Garder LC (1993b) Validation of ISCCP cloud detections. *J Clim* 6:2370–2393
- Rossow WB, Walker AW, Garder LC (1993) Comparison of ISCCP and other cloud amounts. *J Clim* 6:2394–2418
- Shea DJ (1986) Climatological Atlas: 1950–1979. Surface air temperature, precipitation, sea-level pressure, and sea-surface temperature (45° S–90° N). NCAR Technical Note NCAR/TN-269+STR National Center for Atmospheric Research Boulder Colorado
- Shea DJ, Trenberth KE, Reynolds RW (1992) A global monthly sea surface temperature climatology. *J Clim* 5:987–1001
- Smith LD, Vonder Haar TH (1991) Clouds-radiation interactions in a general circulation model: impact upon the planetary radiation balance. *J. Geophys Res* 96:893–914
- Slingo A, Slingo JM (1991) Response of the National Center for Atmospheric Research Community Climate Model to improvements in the representation of clouds. *J Geophys Res* 96:15341–15357
- Stowe LL, Wellemeyer CG, Eck TF, Yeh HYM, Nimbus-7 Cloud Data Processing Team (1988) Nimbus-7 global cloud climatology, Part I: algorithms and validation. *J Clim* 1:445–470
- Stowe LL, Yeh HYM, Eck TF, Wellemeyer CG, Kyle HL, Nimbus-7 Cloud Data Processing Team (1989) Nimbus-7 cloud climatology, Part II. First year results. *J Clim* 2:671–709
- Thompson SL, Ramaswamy V, Covey C (1987) Atmospheric effects of nuclear war aerosols in general circulation model simulations: influence of smoke optical properties. *J Geophys Res* 92:10942–10960
- Trenberth KE (1990) Recent observed interdecadal climate changes in the Northern Hemisphere. *Bull Am Meteorol Soc* 71:988–993
- Trenberth KE (1992) Global analyses from ECMWF and Atlas of 1000 to 10 mb circulation statistics. NCAR Technical Note NCAR/TN-373+STR National Center for Atmospheric Research, Boulder, Colorado
- Trenberth KE, Olson JG (1988) An evaluation and intercomparison of global analyses from NMC and ECMWF. *Bull Am Meteorol Soc* 69:1047–1057
- Trenberth KE, Hurrell JW (1994) Decadal atmosphere-ocean variations in the Pacific. *Clim Dyn* 9:303–319
- Tzeng R-Y, Bromwich DH, Parish TR (1993) Present-day Antarctic climatology of the NCAR Community Climate Model version 1. *J Clim* 6:205–226
- Warren SG, Hahn CJ, London J, Chervin RM, Jenne RL (1986) Global distribution of total cloud cover and cloud type amounts over land. NCAR Technical Note NCAR/TN-273+STR National Center for Atmospheric Research, Boulder, Colorado
- Warren SG, Hahn CJ, London J, Chervin RM, Jenne RL (1988) Global distribution of total cloud cover and cloud type amounts over ocean. NCAR Technical Note NCAR/TN-317+STR National Center for Atmospheric Research, Boulder, Colorado
- Washington WM, VerPlank L (1986) A description of coupled general circulation models of the atmosphere and ocean used for carbon dioxide studies. NCAR Technical Note NCAR/TN-271+EDD National Center for Atmospheric Research, Boulder, Colorado
- Washington WM, Meehl GA (1993) Greenhouse sensitivity experiments with penetrative cumulus convection and tropical cirrus albedo effects. *Clim Dyn* 8:211–223
- Williamson DL (1993) CCM progress report, June 1993. NCAR Technical Note NCAR/TN-393+PPR National Center for Atmospheric Research, Boulder, Colorado
- Williamson DL, Rasch PJ (1989) Two-dimensional semi-Lagrangian transport with shape-preserving interpolation. *Mon Weather Rev* 117:102–129
- Williamson DL, Rasch PJ (1994) Water vapor transport in the NCAR CCM2. *Tellus* 46A:34–51
- Williamson DL, Kiehl JT, Ramanathan V, Dickinson RE, Hack JJ (1987) Description of NCAR Community Climate Model (CCM1). NCAR Technical Note NCAR/TN-285+STR National Center for Atmospheric Research, Boulder, Colorado
- Williamson DL, Kiehl JT, Hack JJ (1994) Climate sensitivity of the NCAR Community Climate Model (CCM2) to horizontal resolution. *Clim Dyn* (in press)
- Williamson GS, Williamson DL (1987) Circulation statistics from seasonal and perpetual January and July simulations with the NCAR Community Climate Model (CCM1):R15. NCAR Technical Note NCAR/TN-302+STR National Center for Atmospheric Research, Boulder, Colorado
- World Meteorological Organization (WMO) (1992) Simulation of interannual and intraseasonal monsoon variability. WMO Report 68, World Meteorological Organization, Geneva, Switzerland